Fossil Record 26 (1) 2023, 51–84 | DOI 10.3897/fr.26.100059

PENSOFT

für Natur MUSEUM FÜR NATURKUNDE BERLIN

The easternmost record of the largest anguine lizard that has ever lived – *Pseudopus pannonicus* (Squamata, Anguidae): new fossils from the late Neogene of Eastern Europe

Erwan Loréal[1], Elena V. Syromyatnikova[2,3], Igor G. Danilov[3], Andrej Čerňanský[1]

1 *Department of Ecology, Laboratory of Evolutionary Biology, Faculty of Natural Sciences, Comenius University in Bratislava, Mlynská dolina, 84215 Bratislava, Slovakia*

2 *Borissiak Paleontological Institute, Russian Academy of Sciences, Profsoyuznaya 123, 117997, Moscow, Russia*

3 *Zoological Institute, Russian Academy of Sciences, Universitetskaya Emb. 1, 199034 St. Petersburg, Russia*

https://zoobank.org/EB01E77B-10FD-4D7F-82C3-6A241635F0FD

Corresponding author: Andrej Čerňanský (cernansky.paleontology@gmail.com)

Academic editor: Florian Witzmann ♦ **Received** 8 January 2023 ♦ **Accepted** 16 February 2023 ♦ **Published** 1 March 2023

Abstract

We here report on new material of *Pseudopus pannonicus*, the iconic and largest-known representative of the lizard clade Anguinae, from several late Neogene localities across Moldova, Ukraine, and regions of the North Caucasus – the last representing the easternmost known occurrence of this extinct species. Today, *Pseudopus apodus*, the last extant *Pseudopus* representative, is found in a variety of habitats ranging from South-East Europe to Central Asia. In the late Cenozoic of Europe, however, several extinct species of *Pseudopus* existed. Among them, interestingly, *P. pannonicus* displayed the largest spatiotemporal range of the genus, occurring from Spain to the North Caucasus and known from the Late Miocene to the Early Pleistocene. Although it has been reported in a plethora of European localities, *P. pannonicus* is a taxon "with several questionings related to its few diagnostic features vs. numerous features shared with *P. apodus*". The elements described here exhibit some variability, but their overall morphology undoubtedly resembles that of previously described material of *P. pannonicus*. The lacrimal from Tatareshty, moreover, represents the first fossil lacrimal reported for *P. pannonicus*. Besides, the fairly complete maxilla with a length of almost 3.7 cm is the largest maxilla ever reported for this taxon, expanding our knowledge of its gigantism. In addition, several features are described and discussed regarding their diagnostic relevance for *P. pannonicus*. The relationship between body size and some of these features was tested statistically. Consequently, two cranial characters and one vertebral feature peculiar to *P. pannonicus* were retained in the diagnosis of the species.

Key Words

Anguimorpha, Miocene, Moldova, North Caucasus, Pliocene, Ukraine

Introduction

This study is part of a larger project aimed at the taxonomical revision of *Pseudopus pannonicus* (Kormos, 1911). Among squamates, Anguidae represent a diversified and widely distributed group of reptiles from which Anguinae is the most derived clade (Augé 2005). Although there have been recent alterations to phylogenetical conceptions that have been stable for decades (e.g., Pyron et al. 2013; Burbrink et al. 2020) and the position of Diploglossidae is still debated (as a subclade of Anguidae, e.g., see Conrad 2008; Gauthier et al. 2012; Pyron et al. 2013; as a distinct clade outside of Anguidae, e.g., see Zheng and Wiens 2016; Burbrink et al. 2020), besides Anguinae three other extant clades are traditionally included in Anguidae. These are Gerrhonotinae, Anniellinae, and the extinct Glyptosaurinae (Sullivan 1979, 2019; Gauthier et

al. 2012; Georgalis et al. 2021). Nowadays, anguines are represented solely by legless forms (note, however, that some fossil taxa were not legless, see Sullivan et al. 1999; Čerňanský and Klembara 2017) included in three genera: the glass lizard *Ophisaurus* Daudin, 1803 from Northern America, Southeast Asia [=*Dopasia* Gray, 1853], and Northern Africa [=*Hyalosaurus* Günther, 1873]; the slow worm *Anguis* Linnaeus, 1758 from Europe and Western Asia; and the Sheltopusik *Pseudopus* Merrem, 1820, from southeastern Europe, the Middle East and Central Asia (Estes 1983; Sindaco and Jeremčenko 2008; Jablonski et al. 2021). All three taxa are also present in the Neogene of Europe. A fourth anguine taxon, *Ragesaurus* Bailon & Augé, 2012, is also known from the Quaternary of Spain. This taxon is known by only a subcomplete dentary and is restricted to one locality on Islas Medas (Catalonia, Spain) (Bailon and Augé 2012). Recently, a fifth taxon - *Smithosaurus* Vasilyan, Čerňanský, Szyndlar & Mörs, 2022 was described from the Early and Middle Miocene of Germany and Austria (Vasilyan et al. 2022). Today, *Pseudopus* is represented only by a single extant species *Pseudopus apodus*. Populations of this species are considered to pertain to three sub-species: *Pseudopus apodus thracius* Obst, 1978 from the western-most part of the geographic range of the species (i.e., coastal Croatia, Greece, Northwestern Anatolia), *Pseudopus apodus apodus* Pallas, 1775 from Asia Minor and Central Asia, and *Pseudopus apodus levantinus* Jablonski, Ribeiro-Junior, Meiri, Maza, Mikulíček & Jandzik, 2021 from the Levant (Jandzik et al. 2018; Glavaš et al. 2020; Jablonski et al. 2021). The genus *Pseudopus* is also known in the fossil record by a plethora of upper Cenozoic remains from localities all across Europe (Klembara 1981; Klembara and Rummel 2018). There are currently four fossil species described: *Pseudopus ahnikoviensis* Klembara, 2012, *Pseudopus confertus* Klembara & Rummel, 2018, *Pseudopus laurillardi* (Lartet, 1851), and *P. pannonicus* (Kormos, 1911) (see Klembara and Rummel 2018). The latter is the largest anguine known with a skull length estimated around 90–100 mm (Estes 1983; Roček 2019). The temporal range of *P. pannonicus* spans the Upper Miocene (MN9) to the Lower Pleistocene (e.g., Čerňanský et al. 2017). As great as the temporal range of this species is its geographic range. Indeed, although most common in Central Europe, the presence of this species has been reported from fossil localities in Spain (Bailon 1991; Blain et al. 2016) to Ukraine (Alexejew 1912; Zerova 1993; Roček 2019) since its original description by Kormos (1911). On the other hand, apart from some notable contributions (Fejérváry-Lángh 1923; Roček 2019), few works tackled the diagnosis of *P. pannonicus* or examined intraspecific variation. In addition, few recent works described various fossil remains that were only identified as indeterminate anguines (Georgalis et al. 2018) or *Pseudopus* sp. (Georgalis et al. 2019a; Georgalis and Delfino 2022) because of preservation issues or restricted material for instance but for which suspicions of affinities towards *P. pannonicus* were hinted at. These reports are from the Balkans area, namely from Late Miocene Greek localities of Ravin de la Pluie and of Maramena, in which is recorded the Miocene-Pliocene transition (Georgalis et al. 2018, 2019a). If the *P. pannonicus* affinities, especially strong from Maramena, suggested by these authors were to be confirmed (see comments later in Results), these reports would thus document the most southward occurrences currently known for that species. The material described by Kormos (1911) originated from the type locality of Polgárdi 2 (Upper Miocene, Hungary) and consisted only of isolated remains, i.e., one premaxilla, one pterygoid and three dentaries of which none was formally established as either the holotype or as lectotypes for this newly described species. Therefore, in accordance with the ICZN (1999), these original specimens are, by definition, automatically and equally designated as the syntypes of this taxon. Several decades later, Estes (1983) referred to one of the most informative dentary from the original material figured by Kormos (1911), i.e., actually a syntype of *P. pannonicus* as emphasized hereabove, as the neotype of *P. pannonicus*:

"Neotype: HGI, dentary (KORMOS 1911, fig. 19); Pliocene, Polgardi, Hungary." (Estes 1983, 141).

More recently, Klembara and Rummel (2018) and Roček (2019) followed that statement from Estes (1983) and referred to that specimen from Polgárdi as a neotype as well, the former authors stating that no collection number was assigned to that particular specimen. However, by the ICZN definition, this specimen cannot be considered as a neotype. It is still unclear why this syntype specimen was referred to as a neotype rather than a lectotype or even an inferred holotype in the first place. It is especially puzzling when the apparent intent behind the words of this author is closest to that of a lectotype usage, and where, in the same publication, multiple uses of lectotypes can be recorded. Prior to the study of Estes, Młynarski (1956) does use the term "holotype" while mentioning the work of Kormos (1911). However, the former author did not specify any specimen in particular: "good photograph of his holotype (fragment of skull)" (Młynarski 1956, 142). Nonetheless, following the ICZN, as neither the exact term of "lectotype" was explicitly used, nor a holotype has been inferred from the original syntypes, the actions of Estes (1983) do not constitute a lectotype designation ([Art. 74], [ICZN] 1999). Thus, no lectotype is currently fixed for *Pseudopus pannonicus*. To alleviate this issue, we here formerly designate a lectotype for the anguine *Pseudopus pannonicus*. The lectotype specimen we select here is the left dentary MÁFI V 2023.1.14.1., the same specimen that was figured in the original description of this taxon (Kormos 1911, 63, Fig. 19 [i.e., the leftmost specimen]) and that was later referred to as a "neotype" by Estes (1983) and Roček (2019). Several features of that dentary are undoubtedly allowing us to identify it as the specimen figure by Kormos, but it should be noted that it has been

slightly damaged since its discovery. Indeed, a few anterior teeth are now broken off and the posterior end of the dentary is lightly damaged as well. In the prior literature, this specimen can be found under the former collection number Ob. 5058, following an older number formatting used previously by the Hungarian Geological Institute in Budapest, Hungary. With the designation of the lectotype here, all other remaining specimens figured by Kormos (1911) therefore lose the status of syntypes and are given the paralectotype status. These include two right dentaries, one premaxilla (currently missing) and a pterygoid (currently missing as well).

In any case, as of today, very few clearly defined apomorphic features are known for *Pseudopus pannonicus*. Yet, many works, including recent ones, have attributed numerous specimens to this taxon with limited argumentation or use of clear apomorphic criteria, sometimes even pointing at the lack of differences with *P. apodus* except for the large size of the bones described (e.g., Młynarski 1956, 1962; Bachmayer and Młynarski 1977; Młynarski et al. 1984; Kotsakis 1989; Tempfer 2009; see Blain et al. 2016 for summarizing comments about the *Pseudopus* material from the Iberian peninsula). Some of these identifications are not necessarily erroneous and are nothing more than the product of their time when differences between both taxa were not yet clearly established. Nonetheless, revisions of these copious amounts of fossils are much desired to update and complete these taxonomic statements with either restricted or no supporting evidence.

Moreover, due to the establishment of other binomina from nearby areas as well as several synonymization actions, the early taxonomic history of this taxon has been subjected to some confusion. Indeed, Bolkay (1913), following the work of Kormos (1911), described the new species *Ophisaurus intermedius*, *Anguis polgardiensis*, and *Varanus deserticolus*. The former two taxa, *O. intermedius* and *A. polgardiensis*, were subsequently treated as junior synonyms of *P. pannonicus* by Fejérváry-Lángh (1923). The third species, *V. deserticolus* is a chimaera taxon, with its syntypes of both a varanid and an anguine (see Georgalis et al. 2017b). At the same time, Alexejew (1912) described *Ophisaurus novorossicus* from the Upper Miocene of Ukraine. According to him, this new species could be distinguished from other *Ophisaurus* (=*Pseudopus*) species based on its tooth count and its stratigraphic position. Similar to the specimens described by Bolkay (1913), the work of Fejérváry-Lángh (1923) led to the synonymization of *O. novorossicus* with *P. pannonicus*. To add to the taxonomical confusion surrounding *P. pannonicus*, because few differences were identified between *P. pannonicus* and *P. apodus* in the past, a rather popular idea started to spread among the palaeoherpetological community. It was suggested that this taxon was in reality a very large morphotype of *P. apodus* (Młynarski 1964; Estes 1983). However, Klembara (1986) stated that he was able to recognize both species in the Early Pliocene (MN 15) locality of Ivanovce, Slovakia. To that can be added the minute report of *Ophisaurus apodus dzhafarovi* (Alekperov, 1978) from the Pleistocene locality of Fatmai village, Azerbaijan, in which incomplete and disarticulated elements from the skull (upper and lower jaws, and frontals), the vertebral column (a mention of over 30 vertebrae, from which 20 are decently preserved), as well as ribs and numerous osteoderms are briefly mentioned. In this publication, it is stated that these fossils were closest to the modern form of *Ophisaurus* (=*Pseudopus*) *apodus*, but that some peculiarities allowed to distinguish this fossil form from the modern one. Following this, a subspecific status was given to that material from Azerbaijan, under the name of *Ophisaurus apodus dzhafarovi*. These peculiarities are given as follows: wider and thicker frontal bones than *P. apodus*, marked ornamentation of osteoderms displaying a network of irregular ridges and grooves, palatine teeth closely packed together. Following the works of Klembara (1979, 1981) in which the validity of the genus *Pseudopus* was reaffirmed, the taxon *O. apodus dzhafarovi* should probably be attributed to the genus *Pseudopus* as well. Very limited information about *O. apodus dzhafarovi* is available in the literature but the brief descriptions provided here (Alekperov 1978) are reminiscent of the tendency toward larger and more robust morphology of *P. pannonicus*. The latter taxon has been reported up until the Early Pleistocene of central and eastern Europe (e.g., Klembara et al. 2010; Čerňanský et al. 2017), but also in Italian (Delfino 2002) and Iberian (Blain and Bailon 2006) localities. The temporal distribution of *P. apodus* overlaps the tail-end of the temporal distribution of *P. pannonicus*, henceforth and without more osteological information and a more detailed stratigraphic position for the material from Azerbaijan, it is a delicate matter to exclude an attribution of the *O. apodus dzhafarovi* material to *P. pannonicus* or to confirm its current attribution. Access to and revision of this material would be much desirable to clarify the status of this taxon. More recently, material from the Upper Miocene of Gritsev (Ukraine) allowed for the study of intraspecific variation and the amendment of the diagnosis of *P. pannonicus*. To conclude, there are currently seven features that are considered to be useful to discriminate *P. pannonicus* from the other species of the genus *Pseudopus*. These features mostly encompass characters from the skull and a single vertebral character (Roček 2019; for mandibular feature, see Čerňanský et al. 2017).

We here describe new material of *P. pannonicus* from nine localities from the Miocene and Pliocene of Ukraine, Moldova, and the North Caucasus where it was previously not documented (or reported but not formerly described), thus broadening the already impressive geographic range of this species to the east. Indeed, some elements from Gaverdovsky and Volchaya Balka herein studied were briefly mentioned by Tesakov et al. (2017). These authors reported the presence of anguines, including *P. pannonicus*, from these Late Miocene localities, namely by the posterior portion of a large braincase, some vertebrae, and osteoderms. These reports were, however, restricted to a short mention of “abundant” material

of *P. pannonicus*. No detailed descriptions or collection numbers were provided. Only a single osteoderm from this material was figured (Tesakov et al. 2017: pl. 7, fig. 15). Pending the clarification of the status of *O. apodus dzhafarovi* (Alekperov 1978) mentioned earlier, in the outcome in which that material from Azerbaijan was to be confidently identified as *P. pannonicus*, hence also becoming the most oriental report of *P. pannonicus*, our occurrences from Volchaya Balka and Gaverdovsky are considered to be the most oriental reports of *P. pannonicus* currently known.

The aims of this paper are as follows: 1) to describe the materials in detail and compare them with previously described material of *Pseudopus pannonicus* including newly rediscovered type material of this taxon from Polgárdi as well as its newly designated lectotype; 2) to compare the material with the other known species of *Pseudopus* with a special emphasis on *P. apodus*; and 3) to discuss the taxonomic implications of our findings.

Institutional abbreviations

DE, Department of Ecology, Comenius University in Bratislava, Slovakia; **GIN**, Geological Institute of the Russian Academy of Sciences, Moscow, Russia; **ISEZ**, Institute of Systematics and Evolution of Animals, Polish Academy of Sciences, Krakow, Poland; **MÁFI**, Hungarian Geological Institute (Magyar Állami Földtani Intézet) in Budapest, Hungary; **ZIN PH**, Zoological Institute, Russian Academy of Sciences, St. Petersburg, Russia.

Geological settings

The following study is reporting on material from several localities scattered across Ukraine, the Republic of Moldova, and the North Caucasus.

Ukraine

A single Ukrainian locality, the Petroverovka village from the Odesa Oblast, is discussed in the present work. It can be found in the literature under the former name of Zhovten (alternatively romanized as Zhoften). It is close to the northern coast of the Black Sea (Fig. 1A). The *Pseudopus* material herein presented originates from deposits of the Lower Maeotian, a regional stage also referred to as Meotian (see Palcu et al. 2019, 36), which correlates to the early-middle Turolian (MN 11–MN 12) of the European continental biochronologic scheme (Fig. 1C). Petroverovka, located near the Novoelizavetovka village, is known for the presence of fossil anguids and snakes (Alexejew 1912; Zerova et al. 1987; Zerova 1993), mammals (e.g., Petronio et al. 2007; Krakhmalnaya 2008; Rosina and Sinitsa 2014), and fishes (Kovalchuk and Ferraris 2016).

Moldova

From the Republic of Moldova, the following localities are studied (Fig. 1B): Kalfa (alternatively Calfa) from the Anenii Noi District, Tatareshty (alternatively Tătărești) from the Cahul District, Lucheshty (alternatively Lucești), Etulia (alternatively Etuliya) from the Vulkanesthy Region, and Khadzhi-Abdul from the Cahul District. From Etulia, it should be acknowledged that herpetological material was retrieved from three local points, respectively Ovrag Nadezhda, Tretiy Ovrag, and Strausovyj Ovrag. The locality of Kalfa is known for the presence of vipers (Zerova et al. 1987; Zerova 1993) and several mammalian taxa (e.g., Delinschi 2014; Čermák 2016; Sinitsa and Delinschi 2016). This locality has yielded the oldest specimens of our material. Indeed, although the exact levels of excavation were not stated, these samples were reported from the Sarmatian regional stage. According to Zerova (1993), Kalfa is more precisely of the middle Sarmatian age (=Vallesian) and correlated to the MN 9b zone. This is the consensus view based on mammalian assemblage compositions (e.g., Koretsky 2001; Krakhmalnaya 2008; Delinschi 2014). However, the exact age of Kalfa has been questioned, as only very few mammal fossils found at Kalfa hold strong biochronological signals (Sinitsa and Delinschi 2016). Moreover, recent studies based on magnetostratigraphic analyses have tentatively suggested a slightly younger age (early MN 10) for Kalfa. As pointed out by some authors (Čermák 2016; Sinitsa and Delinschi 2016; and references therein), the magnetostratigraphic data are more congruent with the overall biochronological markers. Here, we are following the more recent and revised age estimations. Henceforth, the deposits from Kalfa are here treated as from the early MN 10 (Fig. 1C).

The locality of Tatareshty is known to have hosted a faunistic assemblage that is part of the Moldavian Faunal Complex (Redkozubov 2003; Nadachowski et al. 2006). Therefore, the estimated age of the Tatareshty deposits is the late Ruscinian (MN 15) of the European continental scale (Fig. 1C).

The locality of Lucheshty is about 4 km southwest of Tatareshty and of a similar age to Tatareshty. Indeed, the fossiliferous levels examined in Lucheshty have yielded an assemblage of mammals that is also indicative of the Moldavian Faunal Complex. The presence of some taxa, however, has highlighted the possibility of a record of the early MN 16a in Lucheshty. Moreover, remains of fishes, amphibians, turtles, and snakes have also been reported from Lucheshty (Redkozubov 2005; Nadachowski et al. 2006).

The fossiliferous deposits of the Etulia area have been associated with the Moldavian Mammal Complex, i.e., MN 15 (Nadachowski et al. 2006; Baryshnikov and Zakharov 2013). Apart from mammalian remains, fossils of mollusks (Nadachowski et al. 2006 and references therein), amphibians, and reptiles (Szyndlar 1991a, 1991b; Redkozubov 2003, 2008; Syromyatnikova 2017a; Syromyatnikova et al. 2022) have been reported from deposits around Etulia.

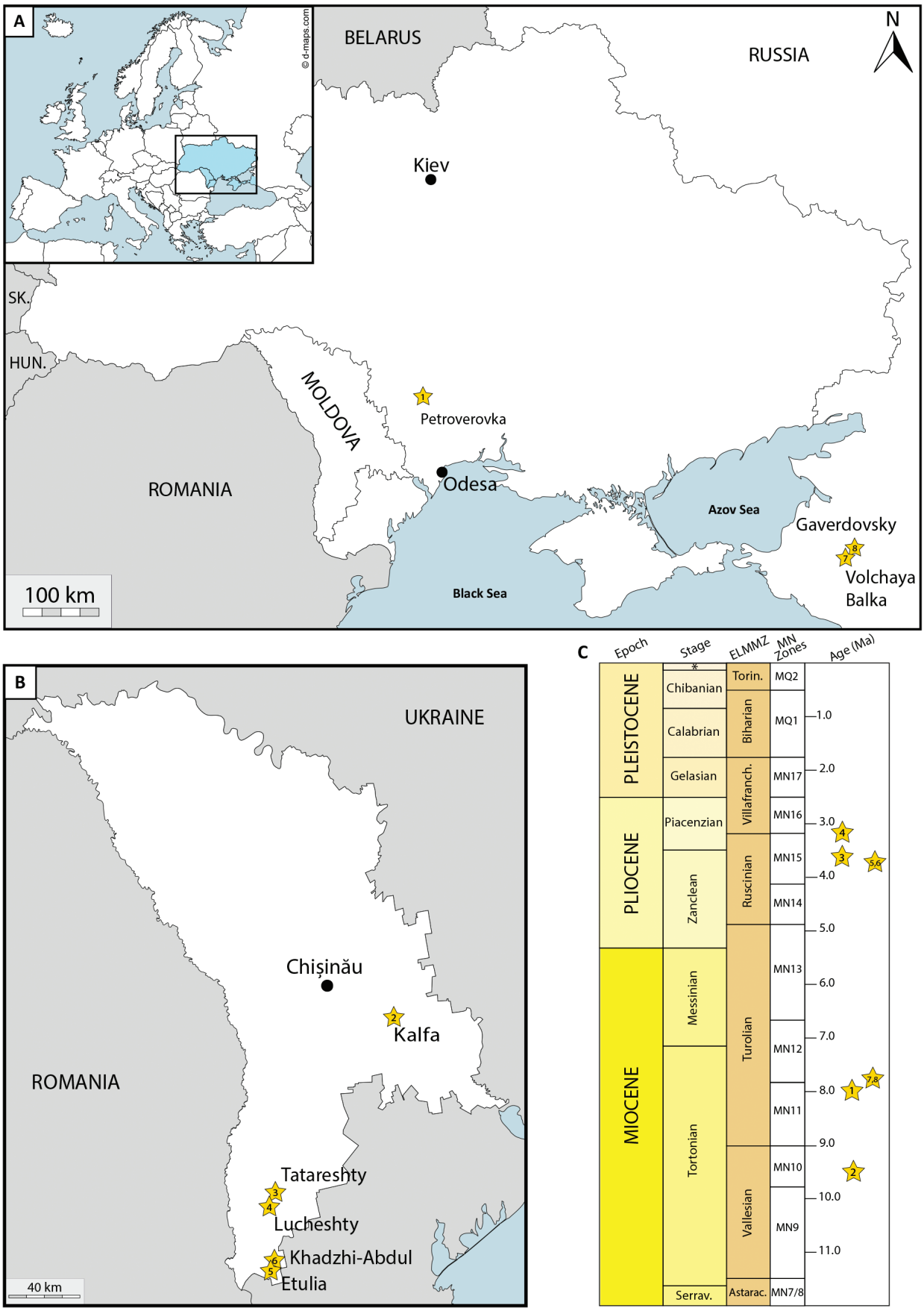

Figure 1. A. Location map of the studied localities. **B.** Close-up on the localities of Moldova. **C.** Stratigraphic position of each locality. Abbreviations: Astarac.: Astaracian; ELMMZ: European Land Mammal Mega Zone; Torin.: Toringian; Serrav.: Serravallian; Villafranch.: Villafranchian; *: Late Pleistocene.

The locality of Khadzhi-Abdul is located near Etulia (Fig. 1B). It was mentioned in the work of Godina and David (1973) under the name of Suvorovo-1, near the Suvorovo village (today named Alexandru Ioan Cuza) from the Cahul district of Moldova. The deposits of Khadzhi-Abdul are from the late Ruscinian, being stratigraphically similar to Etulia.

The North Caucasus

Two localities from the North Caucasus (Russia) are herein presented, viz., Gaverdovsky and Volchaya Balka (Fig. 1A). These localities have yielded palaeobatrachid remains as well as a diverse fauna comprising other amphibians (both caudates and anurans), mollusks, fishes, and reptiles, as well as both micromammal and large-sized mammal taxa (Tesakov et al. 2017; Syromyatnikova 2017b, 2018; Syromyatnikova and Roček 2019). The correlation of several proxies (stratigraphy, ostracod assemblage composition, palynology, mammalian assemblage composition) estimated an age range of 8.1–7.6 Ma (Tesakov et al. 2017) (Fig. 1C), which translates to the early Turolian (MN 11). Although geographically close to one another, Gaverdovsky and Volchaya Balka are associated respectively with a densely forested shore under strong marine water influence and a fresh-water basin with more open vegetation (Tesakov et al. 2017).

Material and methods

The specimens described here were collected on several expeditions in Eastern Europe during the beginning of the second half of the twentieth century. To our knowledge, these campaigns are from the years 1957 (Kalfa), 1959 (Kalfa, Lucheshty), 1961 (Kalfa, Tatareshty, Etulia), 1964 (Etulia), 1965 (Lucheshty), and 1965 (Etulia). One campaign was conducted in Petroverovka with no precise temporal indication, but most likely during the year 1961. More recent campaigns have been conducted in the North Caucasus. Indeed, the material from both Gaverdovsky and Volchaya Balka were collected in 2012.

Specimens examined and terminology

All materials are represented by disarticulated specimens in which the preservation is quite variable, ranging from very poor to fairly complete in some cases. Our samples consist of eight dentaries, five maxillae, four frontals, 11 parietals, one lacrimal, and two fragmentary braincases (for the cranial remains) and 133 osteoderms, 18 vertebrae, and one rib (for the postcranial remains).

The fossil material from Moldova and Ukraine is deposited in the collections of the Zoological Institute of the Russian Academy of Sciences, Saint Petersburg, Russia (collection numbers prefixed by "ZIN PH"), whereas the fossil material from Gaverdovsky and Volchaya Balka is deposited in the collection of the Geological Institute of the Russian Academy of Sciences, Moscow, Russia (collection numbers prefixed by "GIN").

Standard anatomical orientation is used. The anatomical terminology of the individual structures follows, with few exceptions, Meszoely (1970) and Klembara et al. (2014, 2017) for the cranial elements and Čerňanský et al. (2019) for the vertebral elements.

Photography, X-ray microtomography, three-dimensional visualization, and statistical analysis

Specimens were photographed under a Leica M125 binocular microscope with an axially mounted DFC500 camera [LAS software (Leica Application Suite) v.4.1.0 (build 1264)] at the Department of Ecology, Comenius University in Bratislava. Several fossil specimens were scanned using the micro-computed tomography (CT) facility at the Slovak Academy of Sciences in Banská Bystrica, using a phoenix v|tome|x L 240 micro-CT. The CT data sets were analyzed using Avizo v.8.1. and VG Studio Max 3. The type material from Polgárdi was photographed under a scanning electron microscope Thermo Scientific Prisma E SEM housed at the GEOCORE Core Sample, Collection and Laboratory Knowledge Center of the Supervisory Authority for Regulatory Affairs in Rákóczibánya, Hungary. The specimens were left uncoated and photographed under Low Vacuum Mode. The LVD detector was set at various different accelerating voltages, respecting the individual preservation state of the specimens and minimizing unnecessary charging.

Measurements of centrum length (CL) and neural arch width (NAW) follow Szyndlar (1984). The image processing program ImageJ (Schneider et al. 2012) was used for measurements. Statistical analyses were performed with the PAST software (v4.09; Hammer et al. 2001).

Published descriptions and figures of *Pseudopus pannonicus* and *Pseudopus apodus* specimens were used for comparative purposes. Such data were employed as long as there were no ambiguities or doubts associated with these specimens (e.g., descriptions without figures, figures of poor quality, and/or specimens poorly preserved and inappropriate for comparisons). When suited, some of these data from the literature were also included in some of the statistical analyses presented in this work. The analyses made here encompass correlation matrices to understand the various relationships between size measurements, and Student's *t*-tests to compare populations means. Due to the nature of the tests used for the creation of correlation matrices, issues related to multiple comparisons may arise. Thus, to circumvent these issues, a Bonferroni correction is applied when needed and the proper thresholds of significance (i.e., traditionally p-value < 0.05) are adjusted to new corrected values. These values are provided in the section dedicated to the statistical analyses of this manuscript as well as in the

Suppl. materials 1–3. A detailed list of the specimens of *P. pannonicus* and *P. apodus* that were included in the statistical analyses herein presented is provided in the Suppl. materials 1–3 (i.e., Suppl. material 1: *P. pannonicus* specimens, Suppl. material 2: *P. apodus* specimens, and Suppl. material 3: detailed measurements and statistical data for each studied elements).

Data resources

All specimens are catalogued and accessible in the fossil collection of the Russian Academy of Sciences. Digital surface models of the figured fossil specimens are available on Morphosource and Virtual Collections: https://www.morphosource.org/projects/000497477?locale=en.

Results

Systematic palaeontology

Squamata Oppel, 1811
Anguimorpha Fürbringer, 1900
Anguidae Gray, 1825 sensu Gauthier et al. 2012
Anguinae Gray, 1825
***Pseudopus* Merrem, 1820**

***Pseudopus pannonicus* (Kormos, 1911)**
Figs 2–15

Locality, horizon and material. 1. Petroverovka, early-middle Turolian (MN 11 – MN 12): one trunk vertebra (ZIN PH 7/281); four caudal vertebrae (ZIN PH 8/281, 9/281, 10/281, 11/281); and 49 osteoderms (ZIN PH 1-6/281; 12-54/281).

2. Kalfa, Middle Sarmatian age (=Vallesian; MN 10a): five dentaries (ZIN PH 1/277; 2/277; 3/277; 4/277; 5/277); three maxillae (ZIN PH 6/277; 7/277; 8/277); two parietals (ZIN PH 17/277, 18/277); and 57 osteoderms (ZIN PH 9-15/277; 19-68/277).

3. Lucheshty, late Ruscinian (MN 15): one frontal (ZIN PH 2/278); one parietal (ZIN PH 6/278); one fragment of the braincase (ZIN PH 1/278); one presacral vertebra (ZIN PH 7/278); and four osteoderms (ZIN PH 3-5/278; 8/278).

4. Etulia (Ovrag Nadezhda, Tretiy Ovrag, Strausovyj Ovrag local points), late Ruscinian (MN 15): five parietals (ZIN PH 2/279, 3/279, 4/279, 5/279, 6/279), one dentary (ZIN PH 1/279), one presacral vertebra (ZIN PH 7/279), and 11 osteoderms (ZIN PH 8-18/279).

5. Khadzhi-Abdul, late Ruscinian (MN 15): one maxilla (ZIN PH 1/282), two frontals (ZIN PH 2/282, 3/282), two parietals (ZIN PH 4/282, 5/282).

6. Tatareshty, late Ruscinian (MN 15, ?MN 16a): one dentary (ZIN PH 1/280); and one lacrimal (ZIN PH 2/280).

7. Gaverdovsky, Turolian (MN 11): one dentary (GIN 1144/230); one maxilla (GIN 1144/231); one parietal (GIN 1144/232); three trunk vertebrae (GIN 1144/233; 1144/234; 1144/235).

8. Volchaya Balka, Turolian (MN 11): one frontal (GIN 1143/600); one portion of a braincase (GIN 1143/605); five trunk vertebrae (GIN 1143/602; 1143/603; 1143/606; 1143/607; 1143/608); three caudal vertebrae (GIN 1143/601; 1143/604; 1143/609); and 12 osteoderms (GIN 1143/610-621).

Description. Maxilla. Most maxillae available in the material are incomplete except for the right maxilla ZIN PH 1/282 (Figs 2–3). This specimen is fairly complete and very large with a length of 36.93 mm and a height of 11.05 mm, thus making it the largest *Pseudopus*, or anguine even, maxilla ever found. To our knowledge, this is the largest maxilla found among anguids as a whole; see Fig. 2). In any case, all maxillae are robust and relatively large. The exception is GIN 1144/231 which is small and fragile.

The maxilla is anteroposteriorly long and relatively robust with a slight medial curvature at its anterior end. It consists of two major portions: the dental portion bearing the marginal dentition and the dorsally extending nasal process. The nasal process is roughly trapezoidal in shape. It is tall, forming an almost perpendicular wall, although it curves slightly medially at its dorsal extremity. The anterolateral wall of the lacrimal bone was abutting the nasal process of the maxilla where it begins to rise dorsally (i.e., at the level of the lacrimal recess). The anterodorsal margin of this process joins the nasal, whereas its posterodorsal portion broadly overlaps the prefrontal; the latter facet is clearly visible. The dental portion is almost complete, bearing teeth, although a few are missing anteriorly. The tooth row possesses 19 tooth positions (16 teeth are still attached). A short area posterior to the last tooth lacks dentition. In the anterior portion, the maxilla is forked, being divided into two rami. The septomaxillary ramus is thinner and taller than the external ramus. It is also anteromedially flexed and bordered by a small shallow fossa. In medial view, a prominent, concave, and relatively thick, horizontal supradental shelf is present. In the anterior region, a well-developed lip of bone is located on the dorsal surface of the dental shelf. This lamina can be referred to as the septomaxillary lamina (sensu Klembara et al. 2017). The superior alveolar foramen is deep and wide, located at the level of the posterior margin of the nasal process – at the level between the 9th and 10th tooth positions (counted from posterior, see Fig. 2C, D). The adjacent supradental shelf is expanded medially in this area, forming a prominent palatine articulation. The jugal articulation is located in the posterodorsal portion of the posteroventral process, it is wide and deep. The ectopterygoid articulation is present on the posterior end of the maxilla, reaching the level of the 4th tooth position (counted from posterior). In lateral view, the otherwise more-or-less smooth dental portion is pierced by labial foramina in the area ventral to the nasal process. In ZIN PH 1/282, eight foramina are present, being located in a row. However, fewer are present in other maxillae, possibly related to differing preservation states (Fig. 3B, E).

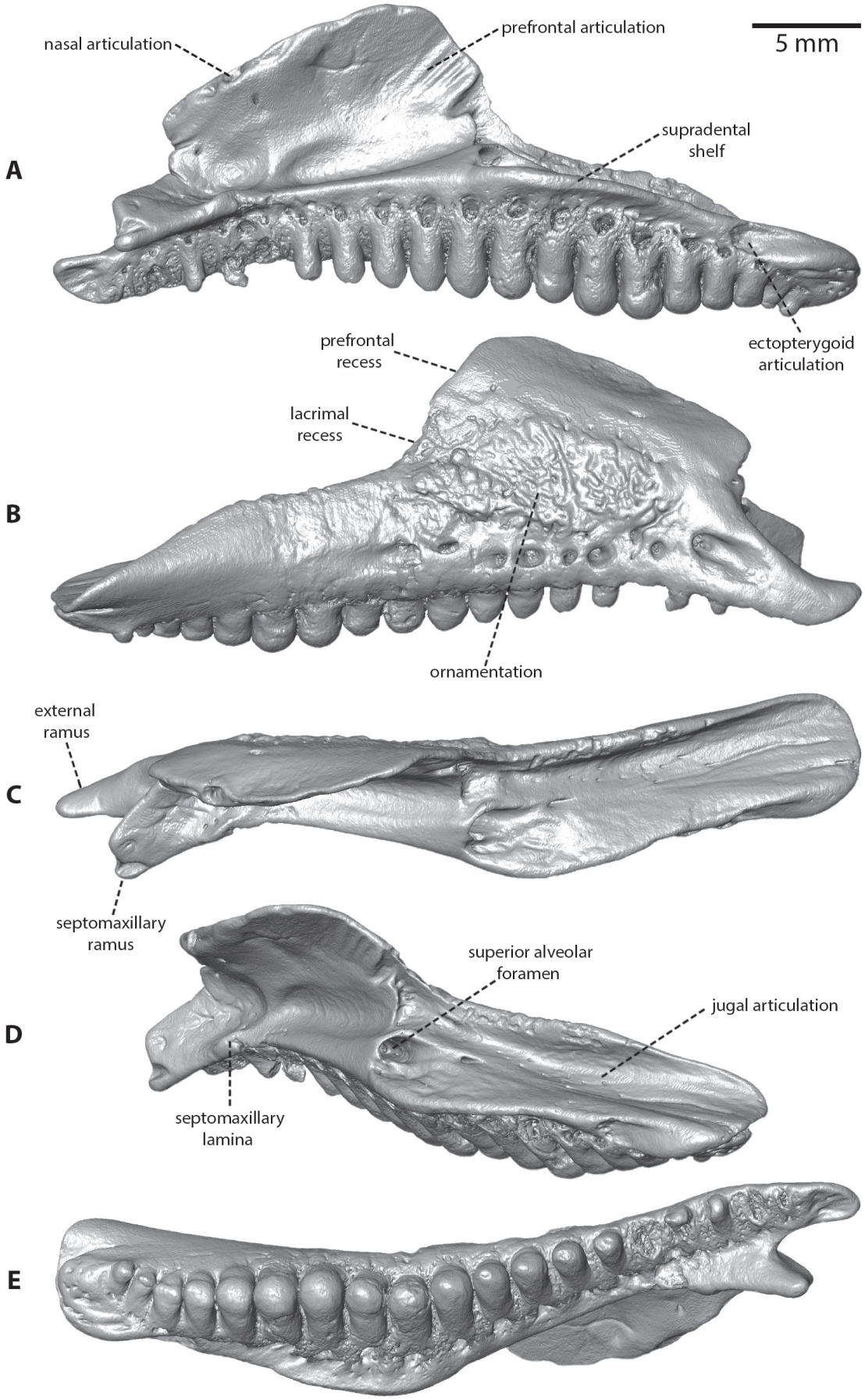

Figure 2. *Pseudopus pannonicus*: virtually segmented model of a right maxilla (ZIN PH 1/282) in medial (**A**), lateral (**B**), dorsal (**C**), posterodorsomedial (**D**), and ventral (**E**) views.

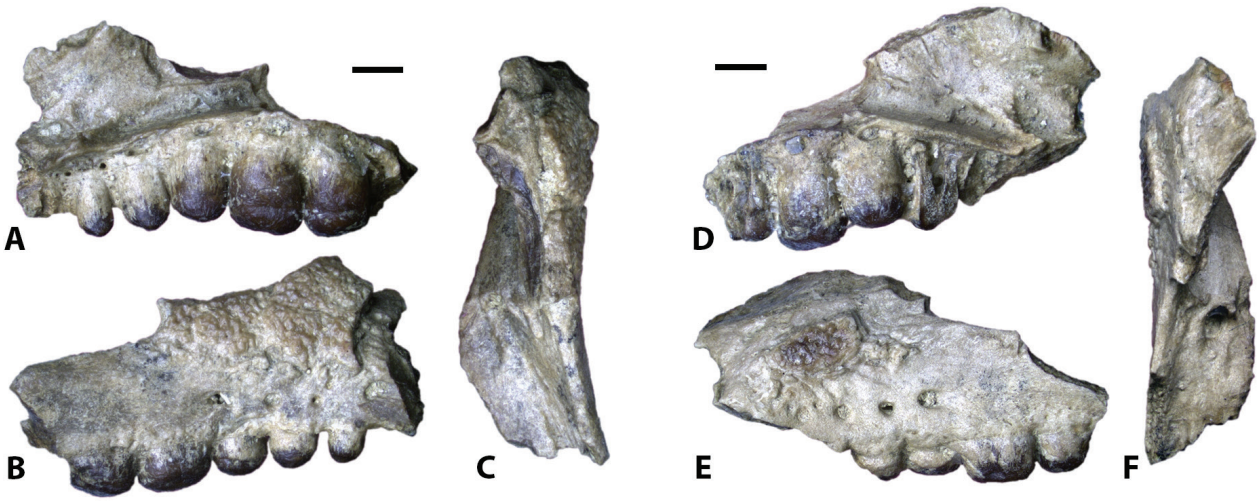

Figure 3. *Pseudopus pannonicus*: right maxilla (ZIN PH 8/277) in medial (**A**), lateral (**B**), and dorsal (**C**) views; left maxilla (ZIN PH 6/277) in medial (**D**), lateral (**E**), and dorsal (**F**) views. Scale bars: 2 mm.

The area above the foramina, which also reaches the ventral region of the nasal process, is covered with several fused, ornamented osteoderms. This ornamentation consists of several irregular ridges and grooves (Figs 2B, 3B, E). The dorsal portion of the nasal process is smooth.

Remarks. The rather small size of maxilla GIN 1144/231, very light lateral dermal ornamentation, and its overall fragility are indications of an early ontogenetic stage, likely of a juvenile and not fully developed individual. In ZIN PH 1/282 with its length of 36.93 mm, the ectopterygoid articulation reaches the level of the 4th tooth position (counted from posterior). This seems to be different from *Pseudopus apodus*, where it reaches the penultimate tooth position (Klembara et al. 2017: fig. 14B). However, this may be subject not only to individual variation but especially to ontogenetic variation, because the ectopterygoid articulation reaches the level of the last tooth in the specimen of *P. pannonicus* from Hambach (see Čerňanský et al. 2017: fig. 7C; its length is 17 mm) and the level of the third position (counted from posterior) in the specimen from Gritsev (Roček 2019: 15C; its length is 24 mm).

Lacrimal. This is a paired bone. The specimen ZIN PH 2/280 is the only lacrimal available in the material (Fig. 4). It is a left element. In lateral view, two distinguishable portions can be recognized. The first, dorsal portion of the lacrimal is roughly rectangular. It is slightly ornamented by a few ridges and grooves. The anterior margin of the lacrimal forms the maxilla articulation. The second, ventral portion of the lacrimal is elongated, extending posteroventrally (Fig. 4A). In medial view, the posteroventrally extending ventral portion of the lacrimal bears a prefrontal articulation.

Remarks. The lacrimal from Tatareshty is the only lacrimal bone reported for *P. pannonicus* (in the fossil members of the genus *Pseudopus*, the partly preserved remains of this element were reported only in *P. laurillardi*, see Klembara et al. 2010). As emphasized by Villa and Delfino (2019a), lacrimal bones are generally quite rare in the fossil record of European lizards, thus making our find noteworthy. However, because of the scarcity of this element in fossil representation and the lack of knowledge about morphological variation, lacrimal bones are of rather marginal interest for fossil identification purposes. This lacrimal generally matches the morphology of the lacrimal known for *P. apodus* (Klembara et al. 2017). The lacrimal from Tatareshty is ornamented, which is a feature that is known in *P. apodus*. However, in the latter species, it is linked to

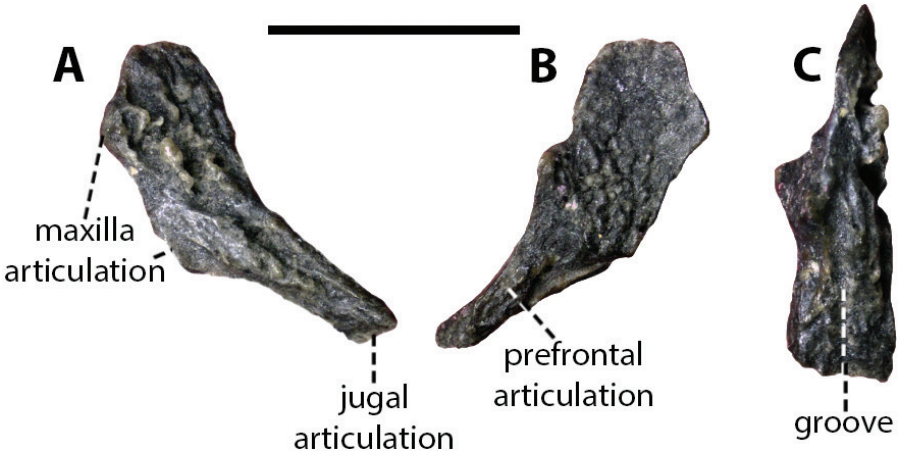

Figure 4. *Pseudopus pannonicus*: lacrimal (ZIN PH 2/280) in lateral (**A**), medial (**B**), and ventral (**C**) views. Scale bar: 2 mm.

size parameters as this condition is known only for large specimens (Klembara et al. 2017). Yet, and interestingly, this lacrimal is relatively small in comparison to that of *P. apodus*. If dermal ornamentation of the lacrimal in *P. pannonicus* is related to size as in *P. apodus*, then the lacrimal of *P. pannonicus* would be among the rare bones to be smaller in *P. pannonicus* than in *P. apodus*. Nevertheless, this lacrimal is the first and only known for *P. pannonicus*.

Frontal. When complete, frontals are large, anteroposteriorly long bones (Fig. 5). In our available material, these paired-bones are all disarticulated and none are found coalesced. The anteriormost portion of the frontal is markedly narrow, extending into a pointed nasal (=anteromedial) process. The anterolateral portion of the process bears the narrow facet for the nasal bone. The facet is sculptured by longitudinal grooves and ridges, indicating strong contact between the frontal and the nasal. The posterior portion of the frontal is the widest. Here, the posterolateral corner of the frontal is distinct and extends into the posterolateral process. In dorsal view, almost the whole dorsal surface is covered by ornamented osteodermal crust, which is fused to the bone. The ornamented surface is even extending far onto the nasal process of the frontal (Fig. 5A, C). The only exception is present in the nasal facet and posteroventral process bearing postfrontal articulation. The ornamentation consists of short grooves, ridges and pits in the central portion of the ornamented surface. The bottoms of some pits are pierced by small foramina. The grooves and ridges diverge from the center to the periphery of the bone, becoming longer (note that this is especially prominent, in the anterior portion of the ornamented surface). The sulci, which separate epidermal osteoscutes (i.e., "shield(s)" of other authors, e.g., Klembara et al. 2010, 2017; Klembara 2012; Čerňanský et al. 2020; Georgalis and Scheyer 2021; Vasilyan et al. 2022, or "ossicula dermalia", e.g., Fejérváry-Lángh 1923; Roček 2019), are less well defined, almost difficult to recognize in some specimens. The incomparably largest osteoscute is the frontal one. It is separated from the frontoparietal and small, posteromedially located interparietal osteoscute (its triangular anterior region overlaps the posterior region of the frontal on the midline; note, however, that it is not preserved in some specimens) by the lateral frontal sulcus and the medial frontal sulcus. The first one is slightly longer than the latter. The lateral frontal sulcus runs in the anterolateral-posteromedial direction, whereas the medial, shorter one has a mediolateral course. The postfrontal articulation extends more posteriorly than laterally.

In ventral view, a large and robust frontal cranial crest can be observed. In its anterior portion, it extends into a rather well-defined and rounded prefrontal (=subolfactory) process. The anteromedial margin of this crest is thin and lightly convex. Posteriorly, it widens and gradually diminishes. It fades out at the posterolateral process of the frontal. Medially, the triangular wedge-shaped parietal tab is indicated by a facet. The anterior portion of the frontal crest is less deep, forming a sharp, medially directed ridge. In the anterior region, lateral to the frontal crest (including its lateral surface), a facet for the prefrontal is located. Its surface is rough and striated. The striation is relatively light on ZIN PH 2/282 in comparison with other specimens. The prefrontal facet is large and occupies anterior two-thirds of the frontal length, and reaches about mid-orbit level. The prefrontal and postfrontal facets are, however, not in contact, so a small lateral portion of the frontal is exposed on the orbital margin.

Parietal. Parietals (Figs 6–7) are medium-sized to large. The parietal is a large azygous element consisting of the parietal table with an ornamented surface and two posterolaterally diverging supratemporal processes. The parietal tab, when preserved, is small. The anterolateral processes are well developed, and their margins are rounded. The lateral margins of the parietal table are more-or-less straight. In dorsal view, the surface of the parietal table can be divided into two areas – a typical

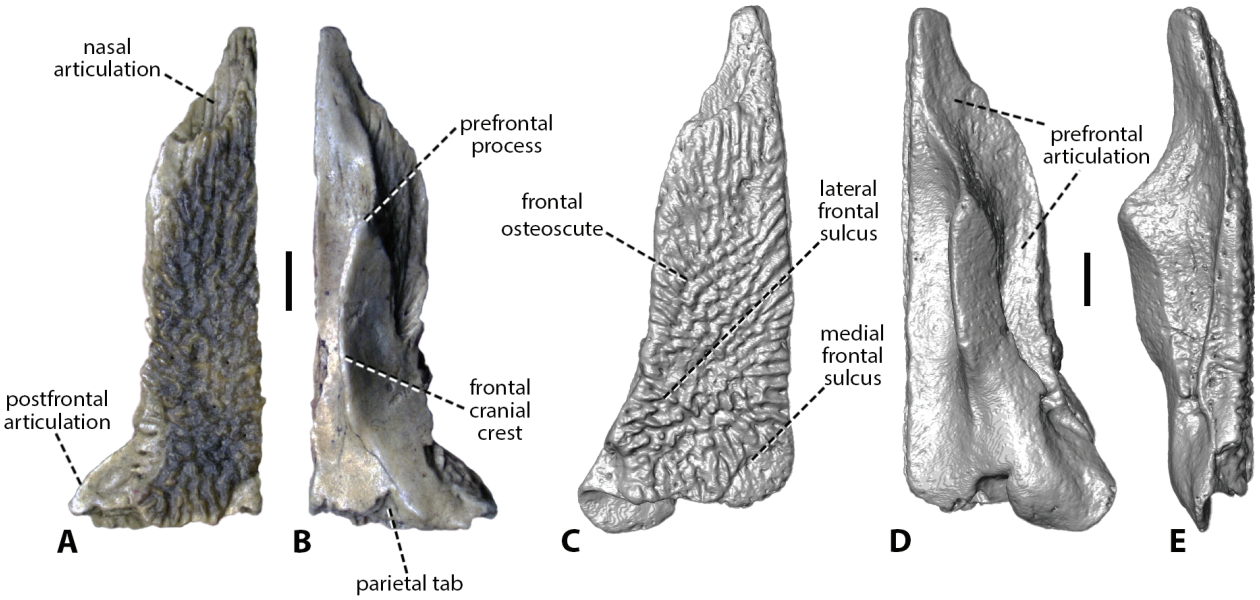

Figure 5. *Pseudopus pannonicus*: photographs of a left frontal (ZIN PH 2/278) in dorsal (**A**) and ventral (**B**) views; virtually segmented model of a left frontal (ZIN PH 2/282) in dorsal (**C**), ventral (**D**), and lateral (**E**) views. Scale bars: 2 mm.

ornamented surface made of osteodermal crusts occupying most of the dorsal surface and a smooth area located posteriorly. The ornamented surface is large and roughly rectangular, being slightly wider than long in large specimens. The interparietal, lateral, and occipital osteoscutes are more or less well-delimited by the interparietal and occipital sulci (Fig. 6G). In the large individual ZIN PH 6/278, however, the sulci are not recognized (see Fig. 7C).

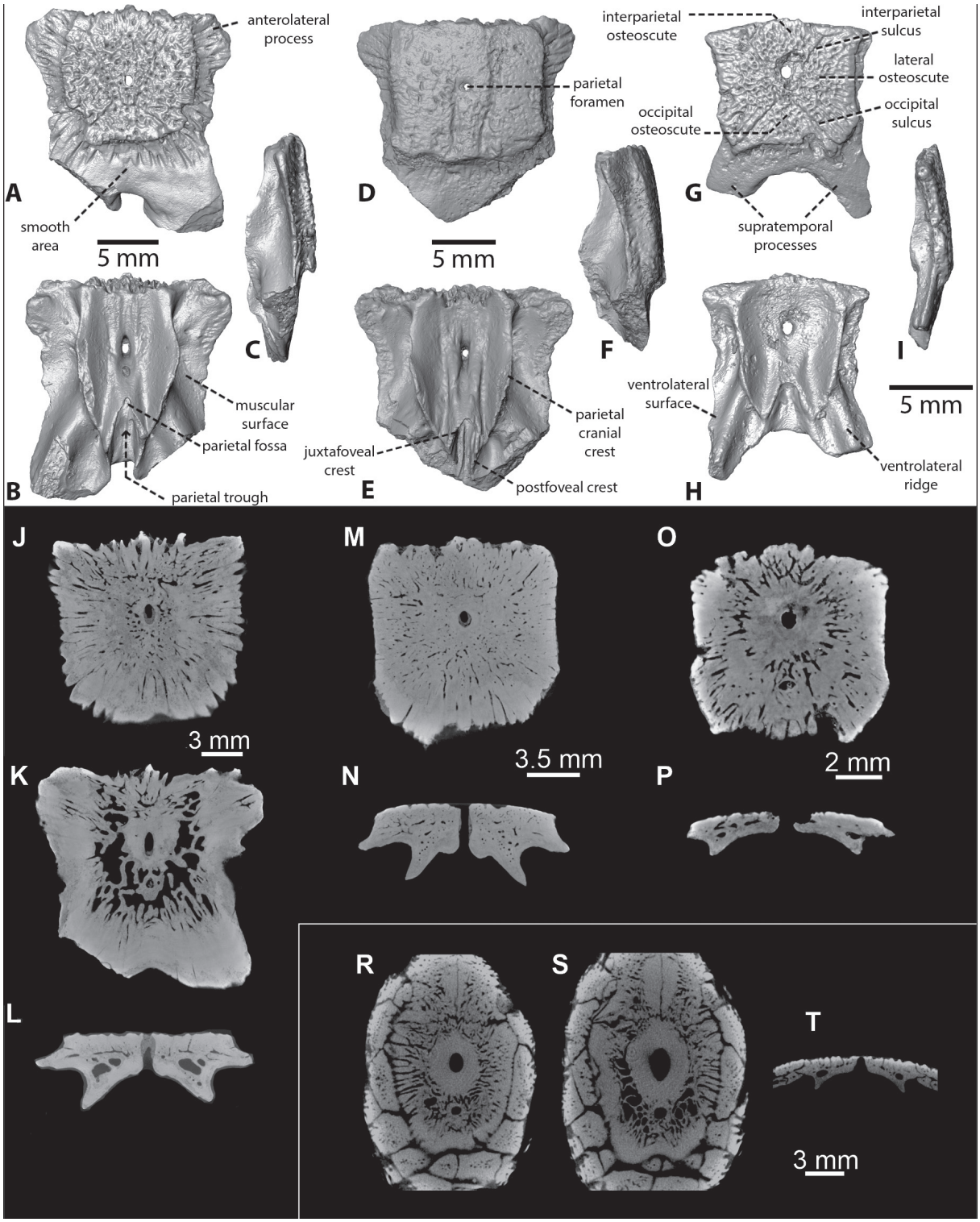

Figure 6. *Pseudopus pannonicus*: virtually segmented models of the parietal ZIN PH 17/277 in dorsal (**A**), ventral (**B**), and lateral left (**C**) views; parietal ZIN PH 18/277 in dorsal (**D**), ventral, and lateral left (**F**) views; parietal ZIN PH 6/279 in dorsal (**G**), ventral (**H**), and lateral left (**I**) views. Virtual slices of the parietal ZIN PH 17/277: axial section at the mid-level of the dorsoventral thickness of the parietal table (**J**), at the ventral level inside of the parietal table (**K**) and coronal section at the level of the parietal foramen (**L**); ZIN PH 18/277: axial section at the mid-level of the parietal table (**M**) and coronal section (**N**); ZIN PH 6/279: axial section at the mid-level of the parietal table (**O**) and coronal section (**P**). Extant *Pseudopus apodus* DE 52, part of the dorsal skull roof: axial section at the mid-level of the dorsoventral thickness of the parietal table (**R**), at the ventral level inside of the parietal table (**S**) and coronal section (**T**).

The dermal sculpture is made of an irregular network of grooves, ridges, and tubercles, being densely distributed. The interparietal osteoscute, when recognized, is pierced by the rounded parietal foramen. The foramen varies in size, being small in some specimens (Fig. 6A), but larger in others (Figs 6G, 7E). The preserved portions of the parietal osteoscutes are the largest relative to others in regard to their size. They are butterfly-wing shaped. As well as the interparietal osteoscute, their anterior portions overlap the frontal. The occipital osteoscute is large. Although its shape slightly varies in the specimens, its posterior margin is usually more-or-less straight. Posteriorly located smooth area of the parietal table is large but shorter than the ornamented surface. The supratemporal processes are not well preserved, being either damaged or broken off in most specimens. In some specimens (e.g., ZIN PH 17/277; ZIN PH 3/279; ZIN PH 6/279; and to a lesser extent ZIN PH 4/282), parts of the supratemporal processes are still preserved. They gradually taper posterolaterally.

Virtual microanatomy and histology. The three micro-CT scans of the parietals revealed a robust bone structure with a very similar internal microanatomy in terms of a vascular network (Fig. 6J, M, O). It revealed relatively large, but not complex meshwork of channels and small cavities. The larger interconnecting vascular cavities of irregular shape are located only in the ventral

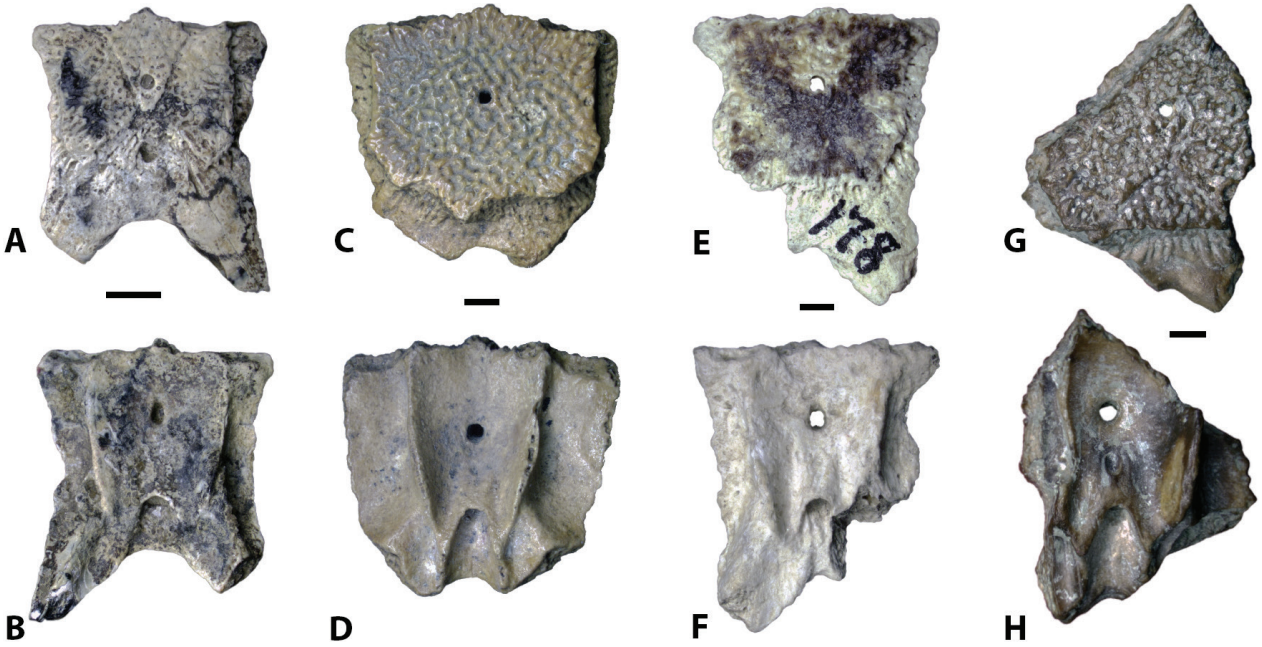

Figure 7. *Pseudopus pannonicus*: photographs of the parietal ZIN PH 3/279 in dorsal (**A**) and ventral (**B**) views; parietal ZIN PH 6/278 in dorsal (**C**) and ventral (**D**) views; parietal ZIN PH 4/282 in dorsal (**E**) and ventral (**F**) views; parietal GIN 1144/232 in dorsal (**G**) and ventral (**H**) views. Scale bars: 2 mm.

In ventral view, the most conspicuous structure is the parietal cranial crest. These crests form sharp walls on each side, so marking the cranial vault. They run generally anteroposteriorly but are slightly convex at mid-length. Lateral to the crest, a distinct muscular attachment surface is present. Its width varies among individuals. In large specimens, its width is equal to the distance between the parietal foramen and parietal cranial crest, whereas in smaller individuals, this distance can be smaller (in some specimens, almost about one-third of the distance between the foramen and the crest). On GIN 1144/232, a small pit is opened posteriorly to the parietal foramen (Fig. 7B, H). The parietal fossa is large and deep, followed posteriorly by the parietal trough. The anterior margin of the fossa is slightly elevated, so this region has a slightly bulged (or swollen) appearance. The fossa is laterally bordered by a sharp juxtafoveal crest. The postfoveal crest is strong and well defined. It is present as a massive ridge continuing from the junction of the end of the juxtafoveal crest and the parietal cranial crest. The supratemporal processes bear the ventrolateral ridges. These ridges are medially bordered by the parietal arch and laterally bordered by the ventrolateral surface. The base of these ridges abuts the lateral wall of the posterior portion of the parietal cranial crest. In lateral view, parietals are slightly externally convex, and the supratemporal processes are flexed posteroventrally.

section of the parietal table of ZIN PH 17/277 (Fig. 6K, L). At this level, they are arranged around the central region, laterally and posteriorly from the parietal foramen (the bony area surrounding the foramen itself is, however, without cavities or channels). From here, a network of thinner interconnected channels extends anterolaterally and mainly posterolaterally (beneath the smooth area). The ZIN PH 18/277 and smaller specimen ZIN PH 6/279 are slightly different - large cavities are absent (Fig. 6M, N, O, P). Here, the extensive, but very fine interconnecting vascular spaces form a dense network. Overall, the condition in *Pseudopus pannonicus* resembles the one in the extant *Pseudopus apodus* (Fig. 6R–T). However,

parietals ZIN PH 17/277 and ZIN PH 18/277 of *P. pannonicus* are distinctly thicker than the one in the latter taxon (see Fig. 6L, N vs. T).

In *P. apodus* - and to a certain degree in the parietals of *P. pannonicus* here - the dorsal portion of the parietal shows numerous foramina which lie inside of pits (for *P. apodus*, see Klembara et al. 2017: fig. 12A). CT coronal section (Fig. 6L, N, P, T) revealed that the foramina represent openings of canals which continue inside to the bone and are connected to meshwork. Note that the finer histological details such as growth marks and cell lacunae of the bone are not visible.

Remarks. Although the dorsal opening of the parietal foramen is varying in diameter in our specimens, when closely observed in ventral view, it seems that the foramina piercing the parietals are of similar size across specimens. Thus, it is possible that this apparent variability in the size of the parietal foramen mentioned here above may likely be explained by differing degrees of osteodermal crust development rather than representing an actual range of individual variation. To support this idea, when observing specimen ZIN PH 6/279 (Fig. 6G, H) in which the osteodermal crust surrounding the parietal foramen is damaged, one can see that both the internal and external openings of the parietal foramen are of the same size. When observing specimen ZIN PH 17/277 in ventral view, a part of the osteodermal crust overlapping the dorsal opening of the parietal foramen can be seen through its ventral opening (Fig. 6B). The small secondary pit described on the parietal GIN 1144/232 (Fig. 7H) is related to individual variation. A similar condition has also been described and discussed for *Pseudopus pannonicus* specimens from Gritsev (Ukraine) by Roček (2019). This can be seen in other taxa such as *Ophisaurus* as well (see Čerňanský and Klembara 2017). As pointed out in more detail by Smith et al. (2018), the apparition of this secondary pit is caused by the "pineal-related cartilage" immediately underlying the bone.

Braincase. The following description is mostly based on specimen GIN 1143/605 as the other specimen from Lucheshty is rather poorly preserved, displaying few features. The specimen from Volchaya Balka is large (Fig. 8). The sphenoid, otic and occipital bones are completely fused in this specimen, and the sutures between the individual bones are hardly distinguishable. Despite its rather damaged right paroccipital process and both alar processes, it is in an overall good shape. In dorsal view, the unpaired supraoccipital lies at the midline and forms the dorsal portion of the posterior braincase, the dorsal part of the inner ear capsule, and the dorsal margin of the foramen magnum. It has a high ascending process with which the ventral crest of the parietal articulates. In lateral view, the process gradually rises dorsally. In dorsal view, the posterior margin of the supraoccipital possesses a wide, V-shaped notch located over the foramen magnum.

In posterior view, the foramen magnum is large, roughly hexagonal. The occipital condyle, which is formed by otooccipital and basioccipital, is heavily damaged. Only its base is present. The latter is flat and trapezoidal (Fig. 8D). Its dorsal margin is much longer than its ventral one. Its lateral margins are rather straight and diverging dorsally. Dorsolaterally from the base of the condyle, there is set of foramina (preserved on the left side): two foramina for hypoglossal nerve (XII) – one is located closer to the occipital condyle, whereas the second more anterolaterally – both located in the depression; here, dorsal to the second one, a foramen for vagus nerve (X) is present and dorsal to it, there is a fourth foramen - potentially for accessory nerve (XI). The otooccipitals are strongly posterolaterally expanded to form the paroccipital processes - only the left one is preserved. It is well-developed, being robust and laterally expanded. A well-developed dorsal ridge runs posterolaterally along the entire dorsal surface of the paroccipital process. This dorsal ridge is slightly curved, mildly convex. The dorsal margin of the spheno-occipital tubercle is well-developed. The spheno-occipital tubercles are rectangular and slightly depressed between their dorsal and ventral margins. These tubercles are expanded ventrolaterally, well below the level of the ventral margin of the occipital condyle. There is a small and medially-pointed extension on the ventral margin of the spheno-occipital tubercles (Fig. 8D). A swelling of the internal surface of the braincase ("bulla tympani" sensu Klembara et al. 2010) is present, well visible inside through the foramen magnum (Fig. 8C, D).

In ventral view, there is a saddle between the basal (spheno-occipital) tubercles, immediately anterior to the area of the occipital condyle. Anterior to the saddle, there is a longitudinal depression running far on the sphenoid. The depression diminishes anteriorly and disappears at the level of the 1/3 of the anterior length of the braincase. The ventrolateral margins of the basal tubercles are prominent, stout.

In lateral view, beginning on the anterior margin of the paroccipital process and continuing strongly onto the prootic is a groove for the vena capitis lateralis (sensu Klembara et al. 2010), which is dorsally bounded by the prootic crest. The prootic crest is well-developed, being sharp. The area ventral to the prootic crest is quite significantly depressed. It is pierced by the fenestra ovalis: the oval window of the braincase in which the footplate of the stapes fits. Ventral to the fenestra is the large occipital recess. These two are separated by a fine, sharp interfenestral crest (Fig. 8H). Anteriorly, immediately below the prootic crest, there is a small foramen for the facial nerve (V). It lies inside the groove for the vena capitis lateralis and is covered by the crest in lateral view. Slightly dorsal to the prootic crest and below the alar process, an additional crest is found. It is running on both sides of the braincase, its course being parallel to the prootic crest. It is not as sharp as the prootic crest but it is sufficiently well defined to be easily observed. More anteriorly, more-or less at the level of the ventral portion of the occipital recess, the bone is pierced by the large posterior opening of the Vidian canal (Fig. 8G, H).

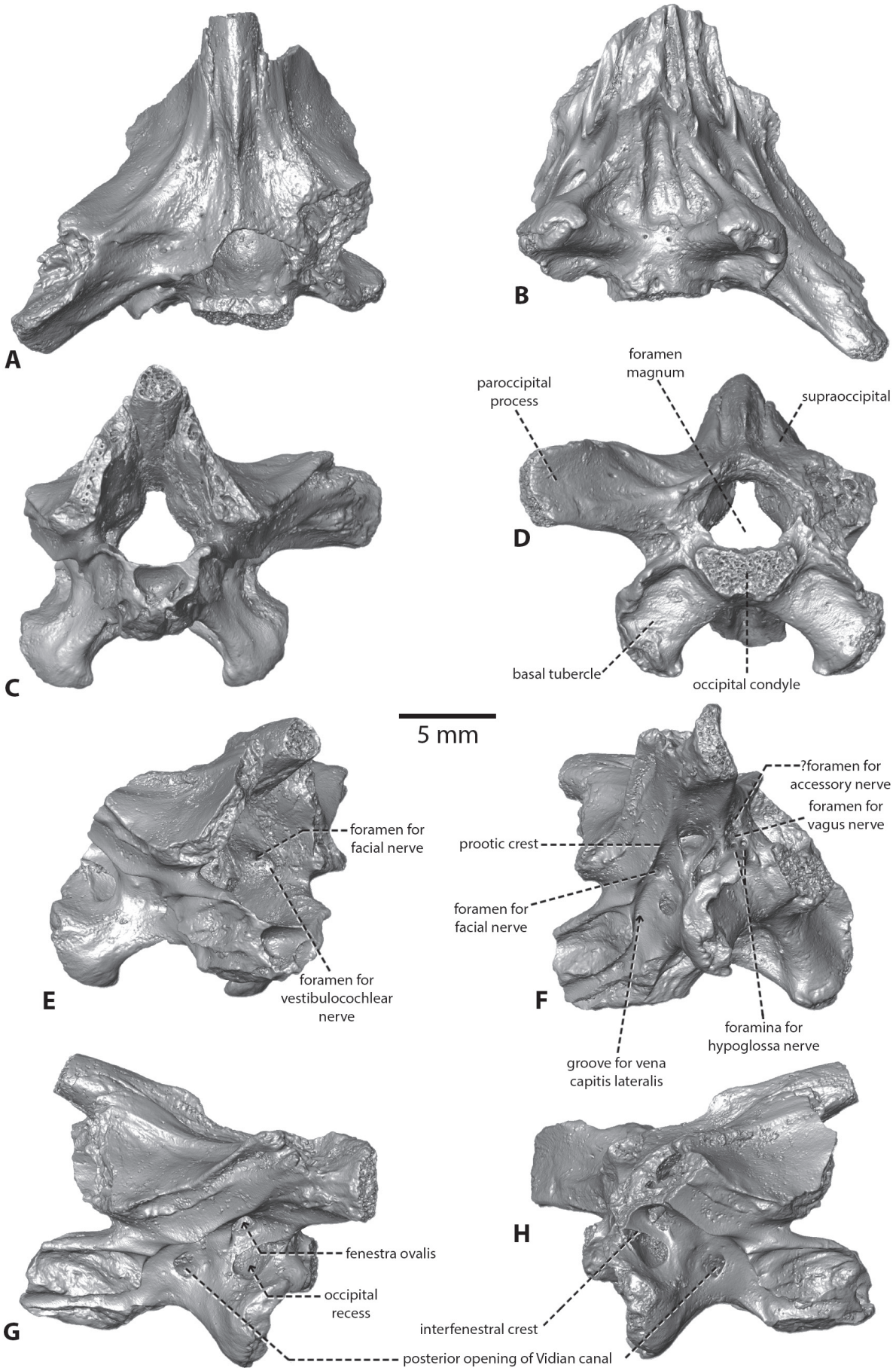

Figure 8. *Pseudopus pannonicus*: virtually segmented model of the posterior portion of a braincase GIN 1143/605 in dorsal (**A**), ventral (**B**), anterior (**C**), posterior (**D**), anterolateral (**E**), posteroventrolateral (**F**), lateral left (**G**), and lateral right (**H**) views.

Anteriorly, the Vidian canal opens lateral to the base of the parasphenoid process (Fig. 8C). The anterior foramen for the abducens nerve (VI) is located directly above the anterior opening of the Vidian canal. A pair of the internal carotid foramina are located centrally, dorsal to the base of parasphenoid process. A sharp crista sellaris is found dorsal to these foramina and runs between the well-developed alar processes. A foramen for a facial nerve opens ventromedially (inside of the braincase) from the prootic crest, inside of the oval depression. In the internal side of this depression, a foramen for the vestibulocochlear nerve (VIII) is also present. The posterior internal area of the braincase is pierced by the perilymphatic foramen. Further posteriorly, the foramen for the vagus nerve and for the hypoglossal nerve are located, piercing the internal posterior area.

Dentary. Several dentaries are available in the material. Because the preservation quality varies among these specimens (Figs 9–11), the following description is mainly based on the best-preserved mature individuals, i.e., specimens ZIN PH 1/277 (Fig. 11A, B), ZIN PH 3/277 (Fig. 9), and to an extent ZIN PH 1/280 (Fig. 10; this specimen represents, however, an immature individual). Tooth rows are mostly incomplete in all specimens, except for ZIN PH 1/280; thus, the total number of tooth positions is difficult to observe.

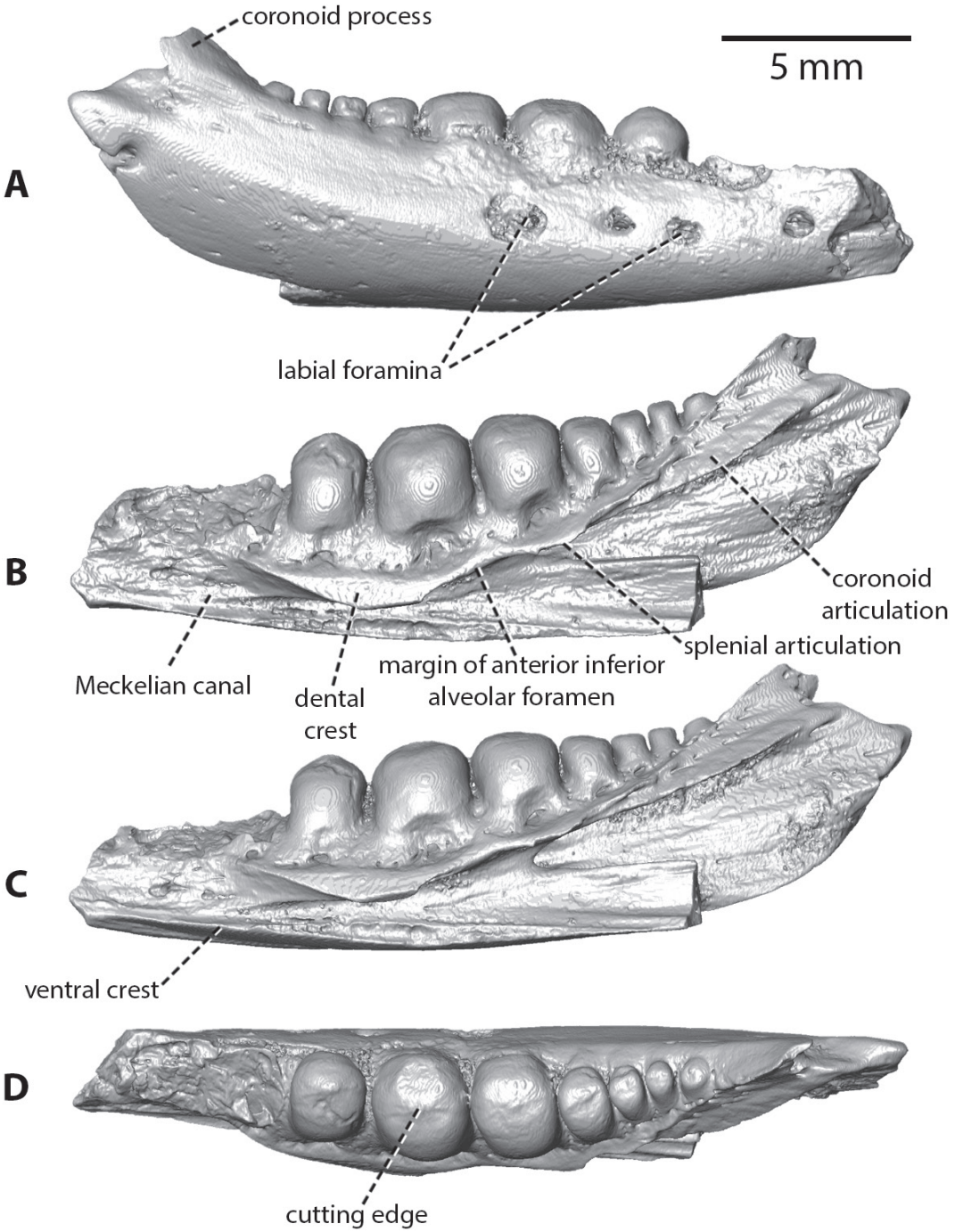

Figure 9. *Pseudopus pannonicus*: virtually segmented model of the right dentary ZIN PH 3/277 in lateral (**A**), medial (**B**), ventromedial (**C**), and dorsal (**D**) views.

Among the best-preserved specimens, ZIN PH 1/280 displays 16 tooth positions (all teeth are still attached except for the small last one; Fig. 10B). The other preserved specimens are large-sized. In medial view, both ZIN PH 1/277 and ZIN PH 1/280 possess their symphyseal region being preserved at the anterior end of the bone (Figs 10B–D, 11A). The symphysis is provided with a kidney-shaped symphyseal facet. The Meckelian canal is fully opened. Anteriorly, it reaches the symphysis in these two above-mentioned specimens, notching it ventrally. Further, the canal continues as a narrow groove, but it widens in the posterior portion of the bone due to the rising of the dental crest in this section. The Meckelian canal is dorsomedially roofed by an almost concave dental crest, whereas it is ventrally bordered by the ventral crest. The ventral crest is more-or-less straight. The ventral and dental crests bear facets for the splenial articulation. In the complete, but immature specimen ZIN PH 1/280, the facets reach anteriorly the level of the 7th tooth position (counted from anterior).

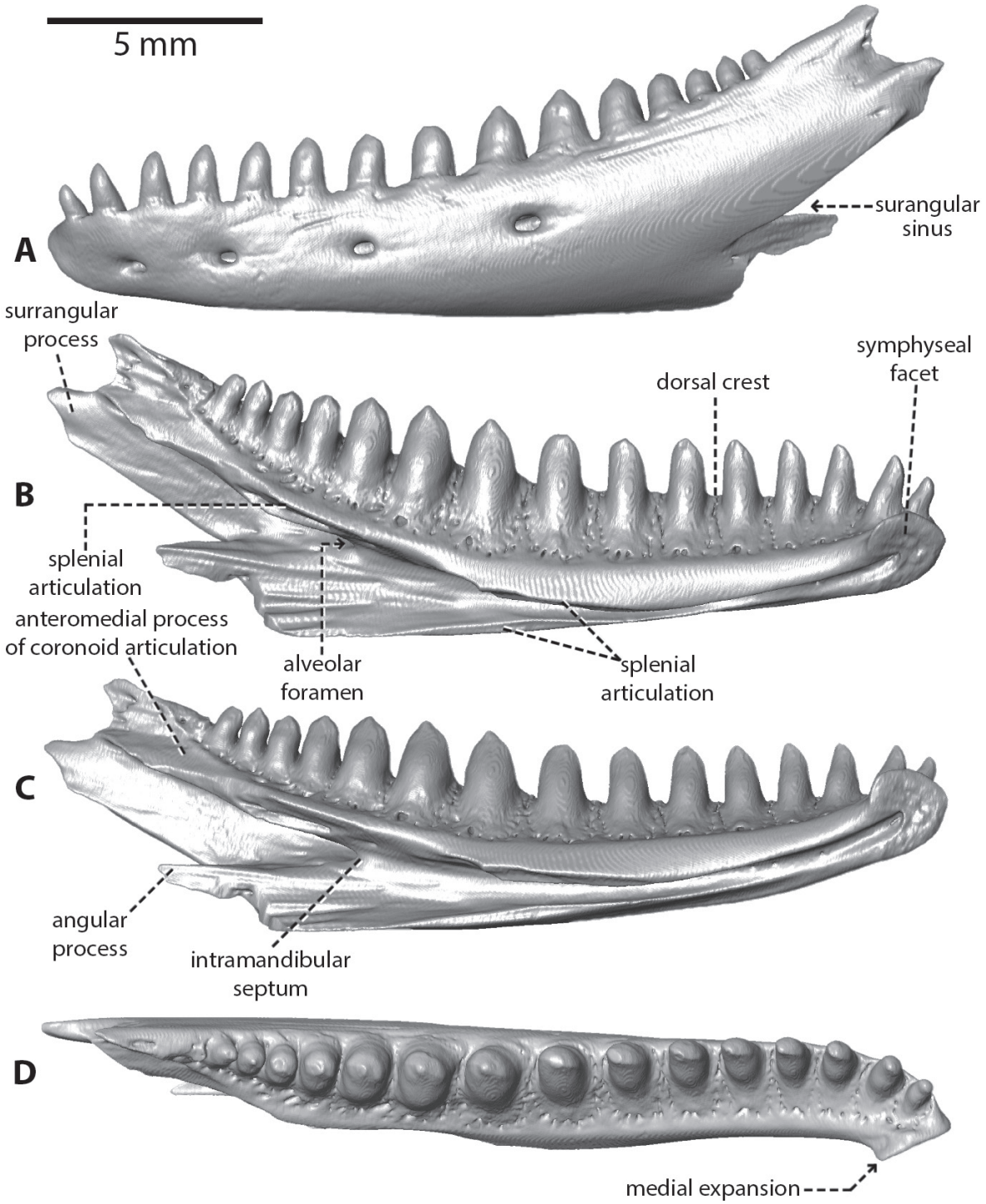

Figure 10. *Pseudopus pannonicus*: virtually segmented model of the left dentary ZIN PH 1/280 (juvenile individual) in lateral (**A**), medial (**B**), ventromedial (**C**), and dorsal (**D**) views.

The anterodorsal margin of the anterior inferior alveolar foramen forms a shallow, elongate notch (the splenial spine is not preserved) at the dental crest, being located at the level of the 5th tooth position in ZIN PH 5/277, at the level between 5th–6th tooth position in ZIN PH 3/277 and at the level of the 6th tooth position in ZIN PH 1/280. The opening of the alveolar canal, the alveolar foramen, is located at the level of the posterior portion of the anterior inferior alveolar foramen (Fig. 11C). The intramandibular septum, which separates the alveolar canal from the Meckelian canal, is almost horizontal. In the posterior portion, the dental crest bears a large facet for an anteromedial process of the coronoid bone. This facet has a rough surface and extends anteriorly to the level of the 4th tooth position (counted from posterior) in the larger individuals and to the level of the 3rd tooth position in ZIN PH 1/280. However, there is a small area that separates the anterior end of the facet from the anterior inferior alveolar foramen, thus the coronoid facet does not reach the foramen. This separating area is difficult to interpret in larger individuals - most likely represents a facet for the splenial (see Discussion). In any case, there is a clear dorsal facet for the splenial posterior to the anterior inferior alveolar foramen in ZIN PH 1/280 – the foramen only interrupts the facet here. This posterior portion of the dorsal facet for the splenial reaches the level of the 3rd tooth position (counted from posterior). The angular process is well-preserved only on ZIN PH 1/280 whereas it is damaged – only the root portion is preserved in other specimens. In ZIN PH 1/280, the posterior tip of this process does not surpass the coronoid process but terminates just anterior to the latter process. The coronoid process is posterodorsally oriented and slightly pointed on several specimens. The surangular process is preserved in some specimens (e.g., ZIN PH 2/277, ZIN PH 1/280). It is large and surpasses both angular and coronoid processes posteriorly (Fig. 11D). The ventral edge of the surangular process bears a distinct notch forming the anterior margin of the anterior surangular foramen. In ZIN PH 2/277 (Fig. 11C, D), the foramen is located completely in the slit in the posteriormost portion of the surangular process, and the slit is posteriorly not completely closed. The foramen seems to be absent in ZIN PH 1/280. The ventral edge of the surangular process of this specimen is rather straight (Fig. 10B). On this particular specimen, the surangular sinus (sensu Klembara et al. 2014; i.e., sinus supraangularis in Roček 1984, 2019), located between the surangular and angular processes, is wedge-shaped.

In lateral view, the otherwise more-or-less smooth surface of the bone is pierced by labial foramina. These form a series located in the mid-line of the bone, and they number four in the best-preserved specimens.

Remarks. The specimen ZIN PH 1/280 is very well preserved and displays a different tooth morphology in comparison to any of the other larger specimens presented here. This specimen displays typical features of *Pseudopus* (Klembara et al. 2014) such as the teeth being rather conical and slenderer with tips slightly curved posteriorly in the anterior half of the dentary, and becoming gradually stouter and more robust in the posterior half. Moreover, the tooth morphology (i.e., thick and conical teeth with pointed apices and posterior teeth being larger and stouter) displayed here is reminiscent of that of juvenile *Pseudopus apodus* (see Klembara e al. 2014). As pointed out in *P. apodus*, the spacing of teeth varies during the ontogeny and as the individuals mature, the teeth of the dentary become more densely spaced (Klembara et al. 2014). Although for a different clade, tooth spacing was also hinted at as a possible juvenile feature by Smith (2011). Henceforth, the general morphology and spacing of teeth is suggesting that ZIN PH 1/280 pertained to a juvenile individual of *Pseudopus*. Klembara (2012) stated that teeth from dentaries of *Pseudopus ahnikoviensis* from the type locality were all devoid of striations. However, as emphasized by Čerňanský et al. (2015, 2017a), this could be linked to intraspecific variability or taphonomy as the latter authors reported for *Pseudopus* cf. *ahnikoviensis* material from the Early Miocene and Middle Miocene of the German localities of Amöneburg (Čerňanský et al. 2015) and Hambach (Čerňanský et al. 2017a) respectively. Similar variability has been shown for *P. apodus* (Klembara et al. 2014). All currently known *P. ahnikoviensis* are confined to the Early and Middle Miocene (MN 3–MN5; Klembara 2012; Čerňanský et al. 2015, 2017; Klembara and Rummel 2018) of Central Europe whereas ZIN PH 1/280 originates from the much younger deposits of Tatareshty

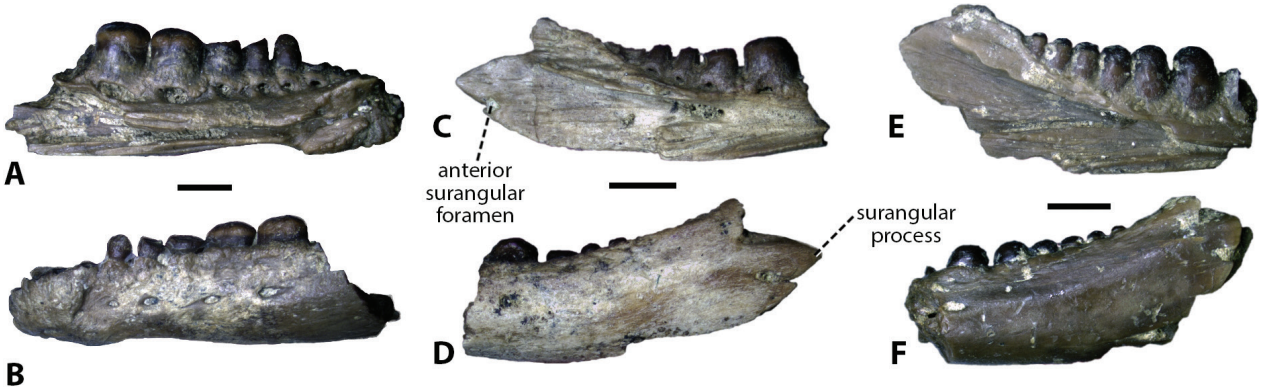

Figure 11. *Pseudopus pannonicus*: left dentary (ZIN PH 1/277) in medial (**A**) and lateral (**B**) views; left dentary (ZIN PH 2/277) in medial (**C**) and lateral (**D**) views; left dentary (ZIN PH 5/277) in medial (**E**) and lateral (**F**) views. Scale bars: 2 mm.

(MN 15). This juvenile specimen is relatively similar in size (20.73 mm in length) to the range known among the adults of *P. ahnikoviensis*. On the other hand, *P. ahnikoviensis* is distinguished from all other *Pseudopus* species by the autapomorphic feature of the dentary in the presence of a surangular spine. Here, ZIN PH 1/280 does not bear a surangular spine but rather a damaged angular process on closer examination. The morphology of the dentary of *Pseudopus confertus* is not currently known. Moreover, this species is solely restricted to a single locality from the Early Miocene (MN3) of the Czech Republic. The dentary of *Pseudopus laurillardi* is known in much more detail than the aforementioned *Pseudopus* species. This species is slightly younger. It is known from Miocene localities ranging from MN4 to MN7/8 (Rage and Bailon 2005; Klembara et al. 2010; Ivanov et al. 2020). One of the most conspicuous and autapomorphic features of the dentary in *P. laurillardi* is the distinct and medially-extending subdental shelf, thus forming a markedly deep sulcus as well as a large medial ridge (Klembara et al. 2010). The latter authors also state that the development of the subdental shelf is affected by ontogenetic processes, being rather narrow in smaller specimens and growing throughout development. Our specimen does not show signs of any subdental shelf, alike *P. ahnikoviensis*, *P. pannonicus*, or *P. apodus*. The posteriormost portion of the dentary of *P. laurillardi* is described as being very short, reaching a length equating to roughly the length occupied by the two posteriormost teeth (Klembara et al. 2010). Here, the posterior portion of ZIN PH 1/280 is notably longer, reaching almost twice that length. It is possible, however, that the immature state of this individual affects the expression of that character. In addition to the various differences with several *Pseudopus* species exposed here, the stratigraphical position of the deposits of Tatareshty is also more congruent with the temporal range of either *P. pannonicus* or *P. apodus*. Finally, ZIN PH 1/280 exhibits an interesting feature in its facet for the splenial. It is most similar to that described for other dentaries of *P. pannonicus* presented here, which appear to have much taxonomical interest (see Discussion), thus comforting the attribution of this juvenile dentary to *P. pannonicus*.

Dentition. Maxillary teeth are small, cylindrical, and slender anteriorly (Fig. 2). These gradually increase in size posteriorly, becoming more bulbous up to the fifth-to-last teeth. Teeth are closely packed. Apices of teeth are lightly striated, both lingually and labially, and pointed. On some teeth, a more-or-less faint anteroposterior cutting edge can be observed. In the dentary, teeth are rather closely packed as well. The most complete specimens show a variation in teeth size along the tooth row. In the anterior portion of the tooth row, teeth are generally more cylindrical and slender, gradually increasing in size and robustness. The largest tooth is located slightly posterior to the mid-length of the dentary. The last four to five teeth are smaller, gradually decreasing in size. In ZIN PH 1/280, the apices of teeth are pointed and slightly striated. A cutting edge is distinct (Fig. 10D).

Trunk vertebra. These presacral vertebrae are relatively well preserved. They are medium-sized to large. These vertebrae are overall rather robust, more compressed rather than elongated (Fig. 12).

They are procelous with the centrum in the shape of a conical frustum. In dorsal view, the vertebrae are constricted at mid-length. Prezygapophyses and postzygapophyses are laterally expanded. The articular facets of the prezygapophyses are oval, slightly elongated in the anterolateral-posteromedial direction, and dorsomedially inclined. The prezygapophyses slightly surpass the level of the anterior margin of the cotyle (e.g., GIN 1143/602), whereas the postzygapophyses do not reach the level of the posterior end of the condyle. The articulation facets of the postzygapophyses are oval, laterally expanded, and ventrolaterally inclined. In lateral view, the prezygapophyses and postzygapophyses are connected by the well-developed interzygapophyseal ridge. The neural arch is lightly depressed medial to the prezygapophyses. The dorsal region of the neural arch slightly rises in height posteriorly. The posteriorly developed neural spine starts to rise at about vertebral mid-length. Unfortunately, it is not complete in any of these specimens, the tip of the neural spine being broken in most specimens (Fig. 12C, H, M, R, W). It thickens posteriorly, thus displaying a hatchet-like morphology in a cross-section. The neural canal is sub-circular, tunnel-like. Its dorsal height is smaller than the dorsal height of the cotyle (for this character, see Čerňanský et al. 2019). In lateral view, the synapophyses are broad, more or less kidney-shaped, and laterally directed. Some specimens display small tubercles located medial to each synapophysis. In ventral view, the centrum is wide but gradually narrows posteriorly - the subcentral ridges are straight and gradually converge posteriorly. The ventral surface is flat. A faint ridge runs anteromedially in some specimens (e.g., GIN 1144/234). Both condyle and cotyle are markedly depressed. The condyle is separated from the body of the centrum by a distinct narrowing, although note that a distinct precondylar constriction (as seen in varanids; e.g., Čerňanský et al. 2022: fig. 5) is absent (Fig. 12B).

Remarks. The two features indubitably allow the allocation of these vertebrae to *Pseudopus* (see Čerňanský et al. 2019): (1) the straight course of the lateral margins of the centrum convergent posteriorly; and (2) the dorsoventral height of the cotyle is higher than the height of the neural canal.

These dorsal vertebrae are robust and large, having short and compressed appearance in comparison to the more elongated vertebrae of *P. apodus*.

Caudal vertebra. The caudal vertebrae are rather poorly preserved. These are medium-sized and rather narrow and anteroposteriorly elongated (Fig. 13).

They are procelous. In dorsal view, the vertebrae are constricted at mid-length. Prezygapophyses slightly surpass the anterior margin of the cotyle. The articular facets of the prezygapophyses are oval, laterally expanded, and dorsomedially inclined. There is a faint ridge

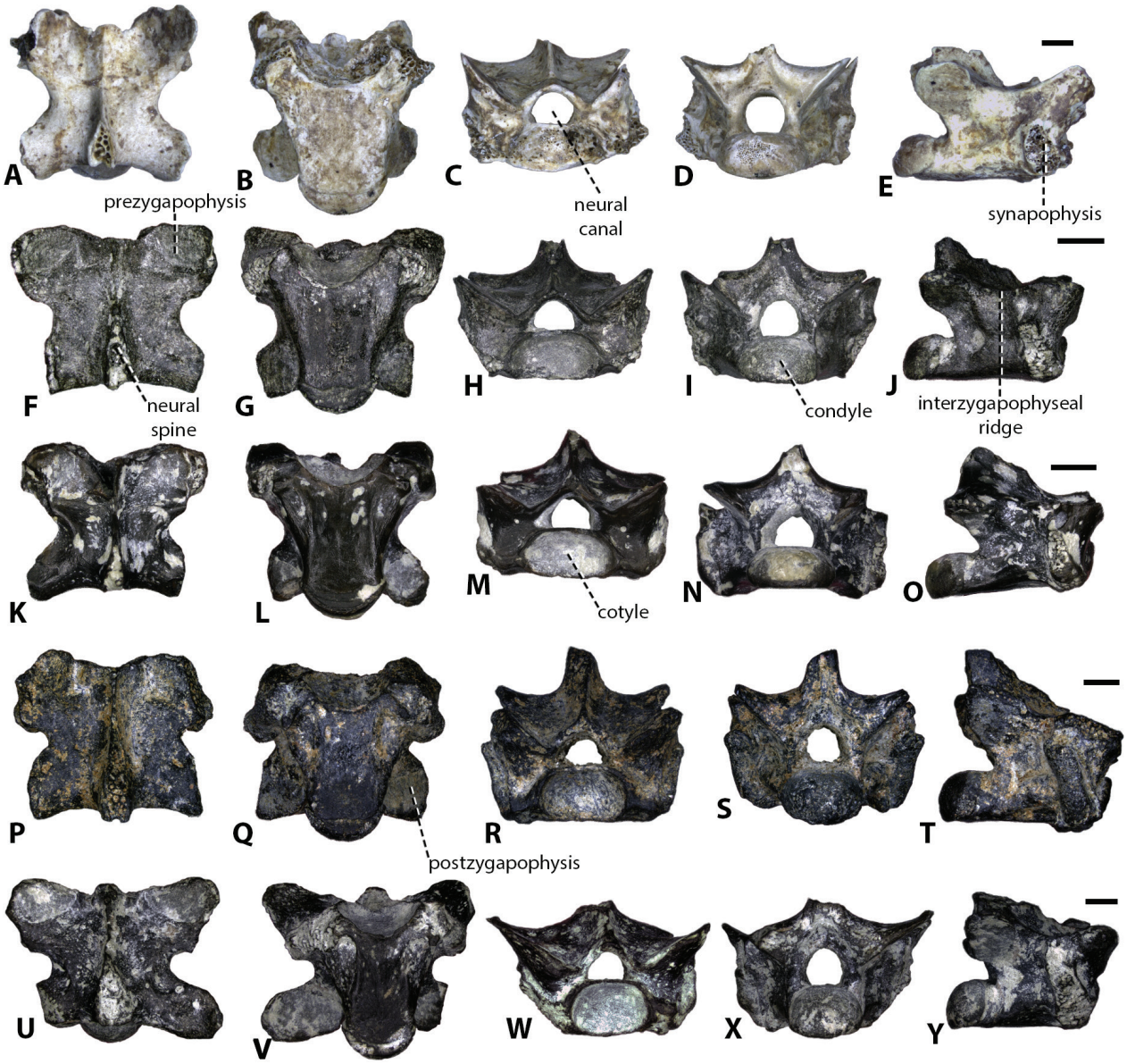

Figure 12. *Pseudopus pannonicus*: trunk vertebra (ZIN PH 7/281) in dorsal (**A**), ventral (**B**), anterior (**C**), posterior (**D**), and right lateral (**E**) views; trunk vertebra (GIN 1143/602) in dorsal (**F**), ventral (**G**), anterior (**H**), posterior (**I**), and right lateral (**J**) views; trunk vertebra (GIN 1144/234) in dorsal (**K**), ventral (**L**), anterior (**M**), posterior (**N**), and right lateral (**O**) views; trunk vertebra (GIN 1143/606) in dorsal (**P**), ventral (**Q**), anterior (**R**), posterior (**S**), and right lateral (**T**) views; trunk vertebra (GIN 1143/607) in dorsal (**U**), ventral (**V**), anterior (**W**), posterior (**X**), and right lateral (**Y**) views. Scale bars: 2 mm.

deriving from the posterolateral corner of the prezygapophyseal facet. These ridges meet medially. In some specimens from Volchaya Balka (e.g., GIN 1143/601; GIN 1143/604; GIN 1143/609), a small apophysis (i.e., the dorsal paraseptal apophysis; Hoffstetter and Gasc 1969, 271) sits atop the level where these ridges meet (Fig. 13P). The articular facets of the postzygapophyses are oval, laterally expanded, and ventrolaterally inclined. The neural spine on these vertebrae is only ever partly preserved. It is slender and pointed. The cross-section of the neural spine is sub-circular. The neural canal is oval, clearly smaller than the cotyle. The subcentral ridges are more-or-less straight. The centrum possesses pleurapophyses. However, only their bases are preserved. These are broad and laterally directed, and gradually narrow distally. The prezygapophyses and pleurapophyses are connected by a vertical wall. The posteromedial margins of the pleurapophyses do not overlap the anterior margins of the postzygapophyses. Some vertebrae (e.g., GIN 1143/604) possess an autotomy foramen at the base of each pleurapophysis, but no transverse autotomic split is present in any of these caudal vertebrae. The centrum is also pierced by several foramina. Only the bases of the haemapophyses are partly preserved on some vertebrae (Fig. 13B, G, L, Q). These bases are posteroventrally oriented. The cotyle and condyle are both depressed. The condyle is slightly smaller than the cotyle.

Remarks. Caudal vertebrae are usually difficult to confidently identify between anguine lizards and are commonly only attributed to indeterminate anguines (e.g., Čerňanský

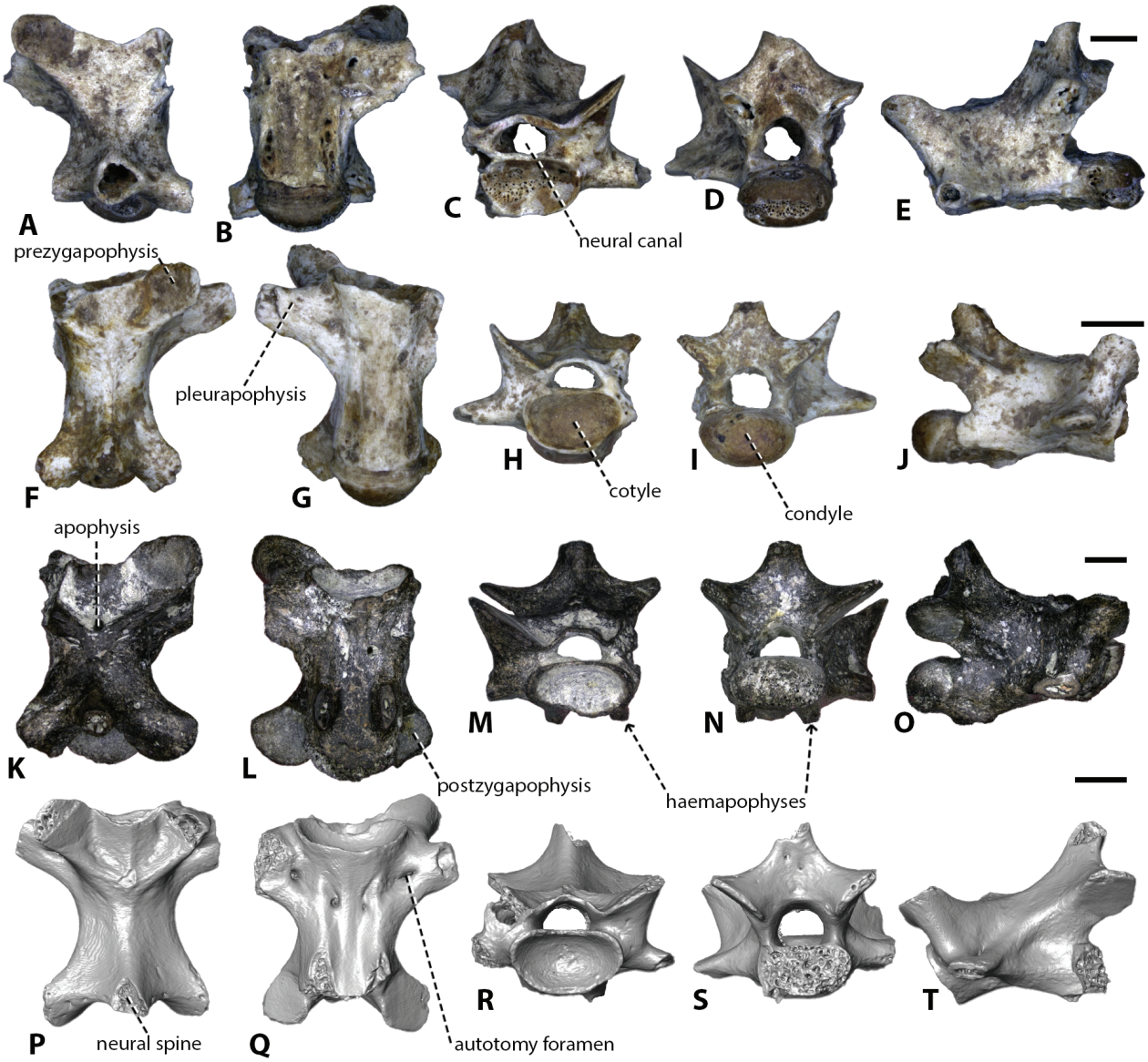

Figure 13. *Pseudopus pannonicus*: photographs of caudal vertebra (ZIN PH 10/281) in dorsal (**A**), ventral (**B**), anterior (**C**), posterior (**D**), and right lateral (**E**) views; caudal vertebra (ZIN PH 11/281) in dorsal (**F**), ventral (**G**), anterior (**H**), posterior (**I**), and right lateral (**J**) views; caudal vertebra (GIN 1143/609) in dorsal (**K**), ventral (**L**), anterior (**M**), posterior (**N**), and right lateral (**O**) views; virtually segmented model of the caudal vertebra GIN 1143/604 in dorsal (**P**), ventral (**Q**), anterior (**R**), posterior (**S**), and right lateral (**T**) views. Scale bars: 2 mm.

et al. 2017; Georgalis et al. 2017, 2018), even though more precise affinities can sometimes be supposed (e.g., Georgalis et al. 2018, 2019a). This becomes even more difficult in the case of large anguid caudal vertebrae as these are strongly similar to those of varanids (Estes 1983; Georgalis et al. 2018). As summarized by Georgalis et al. (2018), some features can nonetheless be used to distinguish caudal vertebrae between large anguids and varanids. Essentially, haemapophyses in the former clade are directly fused to the centrum whereas these are sitting on articulation facets in the latter clade (i.e., pedicles in Georgalis et al. 2018). Additionally, as pointed out by these authors as well, the neural spine also proves useful in distinguishing between anguid and varanid caudal vertebrae, although the distinction is a more delicate matter for the anteriormost caudal vertebrae of anguids which are closer to the morphology exhibited in varanids than the more posterior vertebrae (Georgalis et al. 2018). Among anguids, the neural spine is tube-like and posteriorly inclined whereas, among varanids, the neural spine is rather laterally-compressed and sub-vertical to wholly vertical (Georgalis et al. 2018). In the case of the material presented here, the structures present ventrally in the posterior portion of the centrum are unlikely to be facets for articulation and are, on the contrary, fused directly to the centrum. Moreover, although incomplete in most specimens, the neural spine of the vertebrae of our material are tube-like and rather posteriorly inclined. Therefore, potential varanid affinities among our material can be discarded. Then, as stated previously, identifications of caudal vertebrae among anguines are

difficult and tend to be only referred to as indeterminate anguines, thus rendering our attribution less conservative than usual in comparison. A similar suggestion, although more conservative, was offered by Georgalis et al. (2018) for a limited amount of material (i.e., specimen RP1 299: a single caudal vertebra, likely among the most anterior caudals based on the morphology of its neural spine) from the Late Miocene (MN10) of Greece. These authors referred this specimen to an indeterminate anguine, discarding (although not completely) its possible varanid affinities following a reasoning similar to ours. These authors stated that this specimen could tentatively be attributed to *Pseudopus pannonicus* due to its large size and geographic and stratigraphic positions. Acknowledging that this matter is more sensitive in the case of such limited material, the argumentations of these authors as well as the replacing of that specimen inside a spatiotemporal rationale appear rather sensible. Thus this specimen could warrant a more precise attribution to *P. pannonicus*, hence documenting additional occurrences of that species in the European Neogene. Here, we attribute the caudal vertebrae from our material to the genus *Pseudopus* because none are showing an autotomic split, a feature that is present and well-visible in either *Anguis* or *Ophisaurus* (Hoffstetter and Gasc 1969; Čerňanský et al. 2019). This condition is, however, currently unknown in either *Ragesaurus* and *Smithosaurus* based on the material available (Bailon and Augé 2012; Vasilyan et al. 2022). We refer the vertebrae described here to the species *P. pannonicus* due to the fact that this species is the sole (with the exception of the recently described and rare occurrences of *Ophisaurus* from Lucheshty and Etulia; Syromyatnikova et al. 2022) and most abundant representant of anguines in the localities studied here as evidenced by the additional cranial material described here.

Interestingly and as mentioned in the description above, although some vertebrae are bearing autotomy foramina, none are displaying an autotomic split. To add to these observations, it can be noted that neither "half-vertebra" that could be attributed to autotomized *Pseudopus* elements, nor halves separated post-mortem were found in our material.

Rib. In the available material, a single rib is present (Fig. 14A–C). It is medium-sized. It is lightly bent ventrally as well as lightly compressed anteroposteriorly. The head of the rib is only partly preserved. It displays a more-or-less kidney-shaped articular facet. The anterior process of the proximal end of the rib is preserved whereas its posterior process is not. The distal end of the rib is also lightly damaged. Dorsally, the rib bears a distinct ridge.

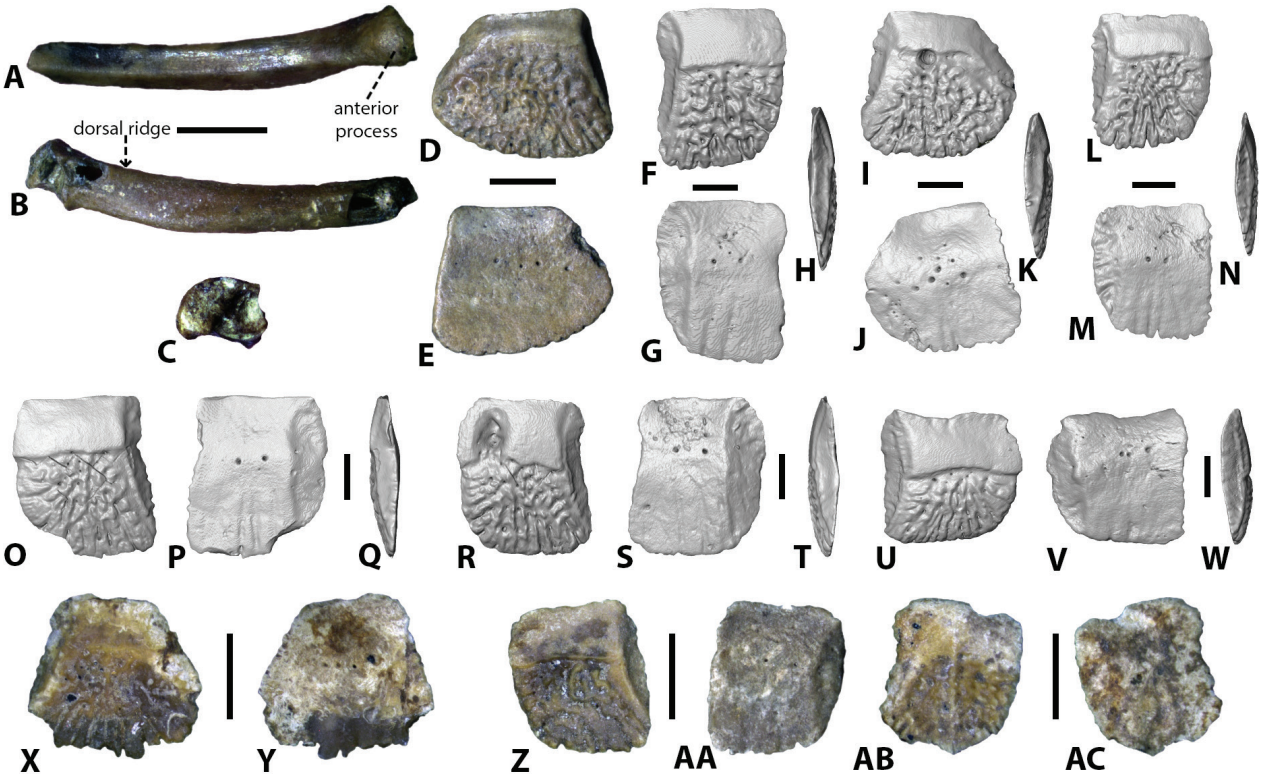

Figure 14. *Pseudopus pannonicus*: rib (ZIN PH 16/277) in anterior (**A**), posterior (**B**), and proximal (**C**) views; photographs of osteoderm from Lucheshty (ZIN PH 3/278) in external (**D**) and internal (**E**) views; virtually segmented model of osteoderms from Kalfa, specimen ZIN PH 9/277 in external (**F**), internal (**G**), and lateral (**H**) views, specimen ZIN PH 10/277 in external (**I**), internal (**J**), and lateral (**K**) views; specimen ZIN PH 11/277 in external (**L**), internal (**M**), and lateral (**N**) views; specimen ZIN PH 19/277 in external (**O**), internal (**P**), and lateral (**Q**) views; specimen ZIN PH 20/277 in external (**R**), internal (**S**), and lateral (**T**) views; specimen ZIN PH 21/277 in external (**U**), internal (**V**), and lateral (**W**) views; photographs of osteoderms from Petroverovka, specimen ZIN PH 1/281 in external (**X**) and internal (**Y**) views; specimen ZIN PH 2/281 in external (**Z**) and internal (**AA**) views; specimen ZIN PH 3/281 in external (**AB**) and internal (**AC**) views. Scale bars: 2 mm.

Osteoderms. Among the herein studied material, osteoderms represent the most common element. Indeed, a total of 133 single osteoderms are recorded. These elements are most abundant in the Kalfa locality and rarest from Lucheshty. In general, some osteoderms are more rectangular and slightly more elongated (e.g., Fig. 14F, R) whereas other osteoderms are more trapezoidal, shorter, and stouter (e.g., Fig. 14D, I). However, all these elements share the following features: rather large, flat, thick, and rather robust. The external surface of the osteoderms can be divided into two distinct areas: a short and smooth gliding surface in the anterior portion and a large, ornamented posterior portion. This ornamentation consists of tubercles mainly in the central part of the ornamented surface and a network of grooves and ridges around the periphery (Fig. 14). Occasionally, pits are found inside these grooves. Some osteoderms have a low, elongate ridge running almost along their middle (e.g., Fig. 14P). In addition, some specimens possess a lateral narrow bevel (i.e., longitudinal crest in Vasile et al. 2021). This feature is, however, certainly most variable as this bevel can be seen on either side of the osteoderms, sometimes both, or rarely on neither side. These different beveling conditions are likely to reflect different placements on the body and can be indicative of left-sided or right-sided osteoderms (e.g., Gauthier 1982; Vasile et al. 2021). In ventral view, osteoderms are rather smooth. Some specimens show light grooves and/or are pierced by foramina (e.g., Fig. 14G, J). In lateral view, these osteoderms are to be rather thick (e.g., Fig. 14H, K).

Remarks. Osteoderms are generally difficult to identify precisely and rarely useful for alpha-taxonomic determinations. Although the morphology of anguid osteoderms tends to be rather generic (i.e., vermicular ornamentation of the external surface; Gauthier 1982; Georgalis et al. 2019b), some possibilities of differentiation between the various anguine genera exist and have been heavily used for fossil osteoderms. For instance, it has been very common to distinguish between osteoderms of *Anguis*, *Pseudopus* and *Ophisaurus*. Indeed, osteoderms of the former are rather small and thin, not rectangular, and devoid of a longitudinal keel (Tesakov et al. 2017; Syromyatnikova et al. 2019; Loréal et al. 2020), whereas osteoderms of the latter two genera are rectangular, larger and both keeled (Čerňanský and Klembara 2017). However, even the keeled feature is not entirely reliable for isolated osteoderms because it is known that some osteoderms of *Pseudopus* can be devoid of this keel, as shown by several authors (Schmidt 1914; Spinner et al. 2015; Vasile et al. 2021). Initially described by Schmidt (1914), the presence of a longitudinal keel in specimens of *Pseudopus apodus* is indeed variable at the individual scale, following a gradient of expression both anteroposteriorly and dorsoventrally across the body. In addition, as pointed out more recently by Vasile et al. (2021), in *Pseudopus*, osteoderms of the dorsomedial region display a medial ridge whereas those of the laterodorsal and lateroventral regions do not. Such results were reaffirmed recently by Spinner et al. (2015). Therefore, the variability described on the presence or absence of a medial ridge is likely reflecting different body topology rather than reflecting actual taxonomical differences. As for the range of variability in the bearing of a lateral bevel, as mentioned above, it can be explained by the positions on the body on which each osteoderm was originally located rather than by taxonomical differences.

Discussion

The allocation of the material to *Pseudopus* is beyond doubt. However, some doubts concerning the distinguishing of *Pseudopus pannonicus* and recent *P. apodus* still exist. In phylogenetic analyses, the two were recovered as sister-taxa and, together with *P. laurillardi* and *P. ahnikoviensis*, formed the clade *Pseudopus* (see Klembara et al. 2019; Vasilyan et al. 2022). The taxonomic allocation of the various elements studied here from different localities to *P. pannonicus* is based not only on the generally large size that characterized this taxon, but also on the presence of several diagnostic features. However, because of the current knowledge of the osteology of *P. pannonicus* and/or the degree of preservation, there are some specimens in this material for which identification to the species level could be questioned (i.e., the lacrimal as it is the first one known in the fossil record for the taxon, vertebrae, especially some that are poorly preserved and osteoderms as these are usually difficult to identify to species-level).

Indeed, several traits are not peculiar to *P. pannonicus* and are shared with other *Pseudopus* taxa, especially *Pseudopus apodus*. The affinities of some of these unremarkable elements with *P. pannonicus* are here justified because of their general morphology, overall large size (similar to, or slightly larger than in *P. apodus*), stratigraphic, and geographic positions. The simultaneous occurrences with other elements more confidently allocated to *P. pannonicus*, in localities where no other anguine reptiles are currently known, are also taken into account. It appears that in the localities herein studied *P. pannonicus* is the most common, sometimes the only, representative of anguine reptiles, thus somewhat strengthening the attribution to *P. pannonicus* of these more generic and non-diagnostic elements. However, it should be noted that some rare occurrences of *Ophisaurus* specimens are known in the Early Pliocene of Moldova. Indeed, two parietals confidently attributed to two distinct *Ophisaurus* species, *Ophisaurus spinari* Klembara, 1979 and *Ophisaurus fejfari* Klembara, 1979, were recently described from Etulia and Lucheshty by Syromyatnikova et al. (2022): the first record of the genus from the Pliocene of Eastern Europe. These findings are quite interesting given how this anguine genus was widely distributed in the Miocene of Eastern Europe and was previously thought to be absent from the Pliocene of this area. Besides, despite these recent rare findings that should not be discarded in any case, very little or no material of anguine reptiles except *Pseudopus*, is known from

Upper Cenozoic fossil sites of Moldova, whereas other squamates such as cf. *Lacerta* sp. or various snake representatives (e.g., Erycidae, Viperidae, or Colubridae) comprise the fossil squamate fauna of the area (Nadachowski et al. 2006). Although it is admitted that there has been a general tendency in the past for lesser attention given to reptile and amphibian fossil assemblages in comparison to other groups such as mammals in Europe (Villa and Delfino 2019b, and references therein), the relatively diverse palaeoherpetofaunas known for these localities would attest that such sampling biases are not the primary explanation for the absence of an otherwise quite common member of vertebrate fossil faunas. The material we document here is interesting as it is supplementing other reports of *P. pannonicus* from that area (Alexejew 1912; Roček 2019) and thus also adds to the range of variation known for this species. Most relevant are both materials from Gritsev (Roček 2019) and especially Novoelizavetovka (Alexejew 1912) as these are well preserved and numerous. Material from the latter locality, originally described as *Ophisaurus novorossicus* and then synonymized with *P. pannonicus* by Fejérváry-Lángh (1923) presents also a notable interest. Indeed, the specimens that have been described and figured from this locality are documenting some of the most common fossil elements in the fossil record of *P. pannonicus* (e.g., maxillae, frontals, parietal, dentaries, vertebrae, osteoderms) in an exceptional state of preservation (i.e., one of the largest specimens from this locality and partially articulated; Alexejew 1912, 30, pl. II., figs 1, 2) but also more scarce elements such as pterygoids, palatines, jugals, quadrates and braincases. Based on the descriptions and figures available, it is difficult to state confidently if the specimens from this locality display some of the characters we present here (e.g., exclusion of the coronoid from the anterior inferior alveolar foramen by the splenial articulation facet of the dentary). The maxillae presented by Alexejew (1912) are bearing rather apparent and well-developed ornamentation, similar to the condition typically observed in *P. pannonicus* that is supplemented by our data and studied further later in this work. The large parietals from that material are displaying wide muscular surface ventrally, almost as wide as the width between the parietal cranial crest and the parietal foramen, a character that is focused on in the present work. The braincase from the Miocene of Novoelisavetovka is exceptionally well-preserved, possibly the best preserved currently known. Unfortunately, its description is most succinct, and the figures provided are limited as well. It would be interesting to see if that specimen also bears, in lateral view, the supplementary longitudinal crest that is located between the alar process and the prootic crest on the specimen from our material and also seemingly on the specimen from Gritsev (specimen NMNHU-P 3390; Roček 2019, 832). Henceforth, as suggested here, this ancient material would benefit most to be revisited, following the many advancements made in regard of the taxonomy of *Pseudopus*, and be revised accordingly to more modern practices and scientific standards.

Intrageneric comparisons with a special emphasis on *Pseudopus apodus*

Currently, *Pseudopus pannonicus* is distinguished from other *Pseudopus* taxa by a limited number of features – some of the previous ones are summarized in the recently amended diagnosis of the taxon (Roček 2019). For a long time, however, *P. pannonicus* has proven to be a rather problematic taxon because of the close osteological similarities to the extant *Pseudopus apodus*. This striking resemblance between the two taxa is something that has long been known and frequently pointed out (Fejérváry-Lángh 1923; Młynarski 1964; Estes 1983; Holman 1998; Roček 2019). It has been the source of several questions about the relationships of *P. pannonicus* to *P. apodus* (e.g., Młynarski 1964), and the true nature of this fossil taxon as a whole (e.g., a fully distinct taxonomic entity, a larger phenotype of *P. apodus*, etc.; see Introduction). On the other hand, Klembara (1986) stated that he was able to recognize both species in the Early Pliocene (MN 15) Ivanovce locality (Slovakia) based on several features, not only their different sizes. Although the material described here as *P. pannonicus* exhibits many similarities with *P. apodus*, there are also several diagnostic features that appear to distinguish it not only from the other fossil members of the genus *Pseudopus*, but especially from *P. apodus*. These features (treated in detail below) are as follows: (1) a more strongly developed ornamentation of the nasal process of the maxilla in comparison to *P. apodus*; (2) well-developed and wider muscular surfaces of the ventral surface of the parietal; (3) splenial facet reaches posterior to the anterior inferior alveolar foramen, thus excluding the coronoid from this foramen; and (4) short and compressed presacral vertebrae in comparison to the more elongated vertebrae of *P. apodus*.

It should be noted, however, that some of these features discussed here or some diagnostic features of *P. pannonicus* are notorious among other groups of squamates for being rather variable in their respective expressions. The variability of some of these features can be explained by the influence of ontogeny and body size (e.g., increasingly marked dermal ornamentation of the prefrontal and frontal among lacertids; degree of concavity of the compound bone among scincids; size-related individual variation of the compound bone in *Lacerta viridis*; Villa and Delfino 2019b). This is mainly the case for character states such as the development of dermal ornamentations, – which in the case of the present study could affect the first character and, e.g., the number of teeth. Although the character states suggested here were either never observed in *P. apodus*, or are somewhat different in *P. apodus*, a correlation to body-size parameters for some of the traits herein discussed cannot be fully discarded. As such, statistical analyses of these features are presented in a dedicated part later in this work.

Maxilla. *Pseudopus pannonicus* is differentiated from other members of the genus, especially *Pseudopus apodus*, by its higher number of labial foramina piercing the

lateral surface of the maxilla as well as by its different number of teeth (Roček 2019). In *P. apodus*, the maxilla is pierced by a maximum of five labial foramina (Klembara et al. 2017). The tooth account of this extant species is up to 14 teeth (Klembara et al. 2014). However, the tooth account of *P. pannonicus* is stated to have a maximum of 12 tooth positions (Bachmayer and Młynarski 1977; Klembara 1986). For example, eleven tooth positions are present in the largest specimen (24 mm) from Gritsev (Roček 2019), and 12 in the smaller specimen (17 mm) from Hambach. The particularly large ZIN PH 1/282 (its length is 36.93 mm, being relatively much larger than the previously described maxillae) described here possesses eight labial foramina (the same as the smaller maxilla from Hambach, see Čerňanský et al. 2017) and displays typical traits of *P. pannonicus* (see Description above for more detail). It has, however, 19 tooth positions, thus markedly surpassing the previously expected maximum of 12 teeth. This is a good example that tooth number in anguines, as in virtually all lizards, is quite variable and also likely to be size related, so these numbers should not be interpreted as absolutes. Therefore, as such a range of variability exists, a restricted amount of teeth might not prove to be the most pertinent of characters to help differentiate taxa (not only to the very least). Drastic variations in the number of teeth should not be overlooked, of course, but in the case of less clearcut differences, a degree of variability should most likely be accounted for.

Laterally, the osteoderms fused to the nasal processes of the maxillae in our material possess a well-developed ornamented surface, better developed than in *P. apodus*.

Frontal. The frontals in our material show clear differences from both *Pseudopus ahnikoviensis* and *Pseudopus laurillardi* while sharing similar characters with *Pseudopus apodus*. The lateral margins of the frontals are straight and gradually converging anteriorly. Additionally, unlike in *P. ahnikoviensis* and *P. laurillardi*, the orbital margins of the frontal are not smooth, but are covered by the ornamented surface. The latter condition is shared with adult individuals of *P. apodus* (Klembara et al. 2017).

Parietal. The parietal shows a combination of characters that are shared across species of the genus. In our *Pseudopus pannonicus* material, the anterolateral processes are rather well-developed, more than in *Pseudopus apodus*, but slightly less than in *Pseudopus laurillardi*. In ventral view, the muscular surfaces of the medium and large-sized specimens are well-developed and large - their width (abbreviated MSw hereafter) approaches, and sometimes equals, the distance between the parietal foramen and parietal cranial crest (abbreviated PCC-MedP hereafter) (e.g., ZIN PH 17/277 and ZIN PH 6/278). In *P. laurillardi* and *P. apodus*, the width of the muscular surfaces is smaller, and narrower (Klembara et al. 2010). In *P. apodus*, the muscular surface is generally half as wide as the distance between the parietal cranial crest and the median plane of the parietal. Comparatively, the observations of our material tend to highlight a width of the muscular surface closer to the PCC-MedP distance. As mentioned previously, this particularity of the parietals of *P. pannonicus* from our material might prove to be diagnostic and will be studied more in-depth later in this work.

Virtual microanatomy. The internal microanatomy in terms of a vascular network is similar in all studied specimens. Small differences might represent individual and/or ontogenetic variations. Interestingly, the meshwork of *Pseudopus pannonicus* with its large interconnected cavities and channels in ventral section of the parietal table (in regard to ZIN PH 17/277) slightly resembles the type present in *Pseudopus apodus* (Fig. 6K vs. S). It should be noted, however, that the parietal ZIN PH 17/277 is clearly thicker and the cavities are much larger and also more variable, irregular in shape. In *P. apodus*, the meshwork in the mid-level is formed by radially diverging channels running to the periphery of the bone. Here, the channels appear to be slightly larger relative to the overall size of the parietal bone than in ZIN PH 17/277. In *P. apodus*, few cavities are present only at the ventral level inside of the parietal table. They are rather small, oval (or box-shaped) and regularly arranged. On the other hand, above mentioned distinct cavities are absent in the large specimen ZIN PH 18/277 and comparative physiological studies of extant anguines are needed to resolve the exact function of the strong parietal vascularization in these lizards. It should be noted that the general type of meshwork in *Pseudopus* slightly differs from the heavily vascularized type present in *Ophisaurus* (the parietal bone appears to be less compact in both axial and coronal sections; see Georgalis and Scheyer 2021: fig. 7). Such small differences in vascular arrangements could indicate some differences in the thermoregulatory function – this might reflect the large body size of *Pseudopus*.

Braincase. The occipital segment of the braincase, although the quantity of our material is strongly limited, shows some interesting features. Braincase elements are not currently known for *Pseudopus ahnikoviensis* and *Pseudopus confertus*, thus hindering any valuable comparisons. Different from *Pseudopus laurillardi* but somewhat similar to *Pseudopus apodus*, the dorsal ridges [i.e., ala otosphenoidea sensu Roček (2019)] are slightly curved. These dorsal ridges are somewhat more prominent than in *P. apodus*. The high ascending process of the supraoccipital crest seems more prominent and more strongly defined than in *P. laurillardi* (although it is partly broken in the only known specimen; Klembara et al. 2010) and in *P. apodus* (Villa and Delfino 2019a). The basal tubercles of our *Pseudopus pannonicus* braincase appear to be somewhat wider than what is known in *P. apodus* (e.g., Villa and Delfino 2019a; CT scans from the Digimorph CT-repository at the University of Texas at Austin, Maisano 2003). The distal ends of the basal tubercles seem also to be somewhat more rounded in appearance than in *P. apodus* (although the difference is admittedly low). This roundness is reminiscent of the condition displayed by *P. laurillardi* (Klembara et al. 2010). In lateral view, there is a mild crest running dorsal to the prootic crest, its course being parallel to that of the prootic crest.

According to our observations, such a crest is not present in *P. apodus*. It is still unclear if this additional crest holds much, if any, taxonomical value but its presence is noteworthy, nonetheless. The Gritsev *P. pannonicus* specimen drawn and figured by Roček (2019) seems to display a similar (although slightly less well defined?) structure but no particular attention has been drawn to it. It is unclear if such a crest is present in *P. laurillardi*¸ although it does seem to be absent. In *P. apodus* and among extant anguids more generally, the ventral surface of the sphenoid is mostly flattened, showing a mild depression in its middle area (Villa and Delfino 2019a). Here, the ventral surface of our specimen is distinctly sunken in its middle area, showing an anteroposteriorly elongated depression. However, braincases of *P. pannonicus* are particularly scarce in the fossil record, and only a handful have been reported, including ours. In the case of the specimen reported from Gritsev (Roček 2019), the ventral surface of the sphenoid is depressed in its middle, but not the extent shown here. With such limited material overall, it is delicate to weigh on the interest of the feature displayed by our specimen. Taphonomic processes could have been at play here and damaged our specimen, for instance. In *P. laurillardi*, such marked depression is not reported (Klembara et al. 2010).

Dentary. The dentary of anguines usually possesses many clear diagnostic features, and this is especially true for *Pseudopus*, which shows the highest number of apomorphies of all anguine genera (Klembara et al. 2014). In contrast to *Pseudopus laurillardi*, the dentaries described here are neither ventrally arched, and nor is the dental crest medially expanded. The surangular spine, a structure present only in *P. ahnikoviensis* within the genus *Pseudopus* (Klembara 2012; Čerňanský et al. 2015), is absent in our specimens. Aside from their overall large size, the dentaries in our material show several similarities with *P. apodus*. The positions of surangular foramen and surangular sinus are similar to that of *P. apodus* contra both *P. laurillardi* and *P. ahnikoviensis*. The angular process of our dentaries does not surpass the coronoid process, a feature characteristic of the genus as a whole (Klembara et al. 2014). The surangular process of our dentaries is similar to that in *P. apodus*. The coronoid processes of our dentaries express some degree of variability in their morphology, which is a tendency also known among *P. apodus* specimens (Klembara et al. 2014). The dentition of our dentaries is also similar to that of *P. apodus*. The number of tooth positions herein observed is well within the ontogenically related range of 11 to 18 teeth known for *P. apodus* (Klembara et al. 2014). Roček (1980, 2019) reported that among ontogenically advanced individuals of *P. apodus*, there were tendencies for the posterior teeth of the dentary to stop being replaced, thus displaying a fused aspect at their bases. This feature should probably be treated carefully when dealing with limited fossil material because of its relationships with ontogenetic series. Nonetheless, the specimens described here tend to be on the lower end of the size spectrum of dentaries known for *P. pannonicus* – namely when compared with specimens from Gritsev (Roček 2019) – and there are no signs of such fusing of teeth in our material. In addition, such fusion has never been described in the literature for specimens attributed to *P. pannonicus*.

There is one dentary character state which might distinguish *Pseudopus pannonicus* from *P. apodus*. In *P. apodus*, the posterior margin of the anterior inferior alveolar foramen is formed by the anteromedial process of the coronoid, a condition not present in the extinct *Pseudopus* species. However, as was previously suggested by Čerňanský et al. (2017a) on the material of *P. pannonicus* from Hambach, a facet for the splenial in this taxon appears to be present posterior to the anterior inferior alveolar foramen – thus, the coronoid is excluded from this foramen. The same condition is present in *P. laurillardi* (see Klembara et al. 2010) and in *P. ahnikoviensis*. In our dentary material, the facet for the anteromedial process of the coronoid clearly does not reach the foramen but is separated from it by an area. This area could be interpreted as a splenial facet (if the splenial attached this area when the mandible was complete). The same condition is present in the lectotype MÁFI V 2023.1.14.1 specimen from Hungary (see Fig. 15) as well as the material from Gritsev (see Roček 2019: "Only the dorsal facet is interrupted by a rounded section that in complete mandible takes part in the formation of a foramen called by Meszoely [1970, figure 4] the anterior inferior alveolar foramen."). In any case, there is a clear facet for the splenial posterior to the anterior inferior alveolar foramen in ZIN PH 1/280.

In summary, we can consider the character state in *P. pannonicus* as different from that of *P. apodus* and support the suggestion of Čerňanský et al. (2017). Note, however, that in juvenile medium-sized individuals of *P. apodus*, the anteromedial process of the coronoid is shorter and pointed, and does not reach the posterior margin of the anterior inferior alveolar foramen. But this points to the fact that the condition in *P. apodus* is peramorphic (see Klembara et al. 2014). In the largest specimen DE 13 of *P. apodus* in Klembara et al. (2014; the length of the mandible of this specimen is 56.8 mm), the condition is slightly different as above mentioned – although the termination of the anteromedial process of the coronoid is rounded and participates in the anterior inferior alveolar foramen, so that the splenial is also not excluded here (see Klembara et al. 2014: fig. 2C).

Trunk vertebra. In our material, the height of the neural canal is lower than the height of the cotyle. This is a character state shared typically with *Pseudopus apodus* as opposed to *Ophisaurus*, one exception being *Ophisaurus harti* as highlighted by Čerňanský et al. (2019). In addition, the trunk vertebrae described here appear to be wider, being markedly less elongated, than the trunk vertebrae of *P. apodus*. Trunk vertebrae of the latter taxon are somewhat elongated, as highlighted by their centrum length and neural arch width ratio of 62% (Čerňanský et al. 2019). Here, our material is associated with a CL/NAW ratio closer to 90%. This characteristic will be developed more thoroughly later in this work.

Figure 15. The lectotype, MÁFI V 2023.1.14.1. (former Ob. 5058) of *Pseudopus pannonicus*: left dentary from the Late Miocene of Polgárdi 2, Hungary, in medial (**A**) and lateral (**B**) views.

Caudal vertebra. Caudal vertebrae are unknown for *Pseudopus ahnikoviensis* and *Pseudopus confertus* (Klembara 2012, 2015; Klembara and Rummel 2018), whereas a few, albeit not particularly informative, are known for *Pseudopus laurillardi* (Klembara et al. 2010) and a handful are known for *Pseudopus pannonicus* (including the ones presented here; e.g., Alexejew 1912; Klembara 1986; Roček 2019). Noteworthy is the fact that several caudal vertebrae have been reported as either indeterminate anguines or *Pseudopus* sp. but with hints of potential affinities towards *P. pannonicus* (e.g., Georgalis et al. 2017a, 2018). As mentioned briefly earlier in this work, some specimens with such suspected affinities could potentially be reassigned to *P. pannonicus*. As it has been also emphasized previously, the distinction of anguine taxa based solely on osteological features of caudal vertebrae is difficult and a traditionally more conservative approach is preferred by only referring such specimens to indeterminate anguines (Čerňanský et al. 2017a, 2017b; Georgalis et al. 2018). Unfortunately, few to no features (supposing there are any) allowing for the confident distinction between *Pseudopus* species, especially *P. pannonicus* and *P. apodus* are currently known. Thus, additional insights from other rationales (e.g., stratigraphy, geography, compositions of fossil assemblages, etc.) need to be considered to argue for any particular specific identification. Here, our material is most similar to the morphology of caudal vertebrae known in *Pseudopus*, namely *P. apodus*. Indeed, these are generally narrower than the presacral vertebrae observed here. No autotomic split is apparent despite the presence of autotomy foramen in some specimens. This material is also rather similar to better preserved caudal vertebrae from Gritsev (Roček 2019) or other similarly preserved specimens (e.g., Alexejew 1912; Bachmayer and Młynarski 1977; Klembara 1986; Venczel 2006).

Osteoderms. The osteoderms allocated to this form are large and thick. As mentioned earlier, due to the difficulties of alpha taxonomic determinations linked to osteoderms, an identification as an indeterminate anguine would be totally admissible because of the vermicular ornamented surface. Here, in the case of our material, we argue that the features displayed by these osteoderms exclude an *Anguis* identification, thus leaving *Ophisaurus*, *Pseudopus*, *Ragesaurus*, and *Smithosaurus* as the remaining anguine taxa that these osteoderms could be attributed to. The osteoderms of either *Ragesaurus* or *Smithosaurus* are still unknown as these taxa are known only by limited

material respectively from the Quaternary of Spain (Bailon and Augé 2012), and from the Early and Middle Miocene of Germany and Austria (Vasilyan et al. 2022). The larger size and robustness of these elements seems to be more congruent with *Pseudopus*. An identification of some of our osteoderms to *Ophisaurus* is not necessarily excluded as two different members of this genus have been reported recently by Syromyatnikova et al. (2022) in both Lucheshty and Etulia, coexisting with *Pseudopus* representatives (this study). However, because of the age of these specimens, their size, as well as the relative scarcity of *Ophisaurus* material from the Pliocene of Eastern Europe (i.e., two damaged parietals) in comparison to the amount of material confidently attributed to *Pseudopus* here, we tentatively identify our osteoderms from Lucheshty and Etulia, and the remaining specimens from Kalfa, Petroverovka, and Volchaya Balka, as belonging to *Pseudopus* and more particularly *Pseudopus pannonicus*, due to their robustness and thickness. Although the morphology of these osteoderms is roughly similar to those known in *P. apodus*, the osteoderms of our material are generally markedly thicker.

Statistical analyses

Dermal ornamentation of the maxilla. The preservation of three of the five maxillae available in the material allows observation of the size of the ornamentation of the nasal process. Besides these three specimens, data from nine maxillae of *Pseudopus pannonicus* described and figured in the literature were added. Specimens, either from our samples or the literature, with heavily damaged or missing nasal process, have been excluded from the samples tested, leaving thus only specimens suited for the analyses conducted here. The height and width of the ornamented surface and the total height and width of each maxilla are measured (Fig. 16) and a correlation matrix was established.

This matrix (Fig. 17) shows with statistical significance (i.e., p-values less than the Bonferroni correction) on one hand that both the width and height of the dermal ornamentation are positively correlated to each other, and that the overall width and length of the maxillae are positively correlated to each other as well. On the other hand, the dimensions of the ornamentation are also positively correlated to the size of the maxilla, although slightly less to its height than its length. However, there is only statistical significance for the relationship between the ornamentation dimensions and the total height of the maxillae. Our sample size is admittedly rather small and more well-preserved specimens would be most welcomed but our results are nonetheless interesting regarding intraspecific variability. Although there is a seemingly positive correlation between the development of the ornamentation of the nasal process of the maxilla and the body size, our data only really support a correlation with the height of the maxilla (i.e., stronger ornamentation on more developed nasal process and vice versa). This suggests that the ornamentation of the nasal process is a character that is subject to changes throughout the ontogeny of *P. pannonicus* and that older individuals would tend to display larger and more developed dermal ornamentation than younger, less mature, individuals. The smaller individuals of our material as well as the ones from the literature used here for comparisons tend to display a degree of ornamentation at least similar to that of adults of *Pseudopus apodus*, if not more strongly developed, whereas larger individuals tend to bear more developed ornamentation. Studies focusing on this feature of the maxilla of *P. apodus* throughout different ontogenetic series would be most interesting to compare the intraspecific variation among these two taxa. Based on the pattern that our results are suggesting, it could be assumed that the ornamentation of the nasal process of the maxilla is also subject to ontogenetic changes in *P. apodus*.

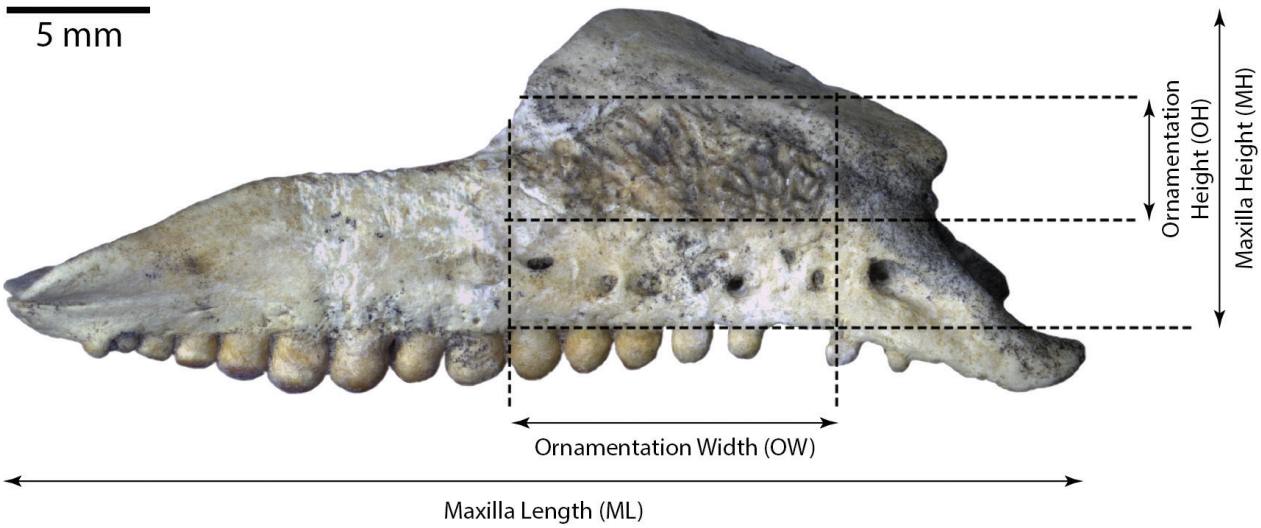

Figure 16. Measurements of the maxilla of *Pseudopus pannonicus* used in statistical analyses in the present work (here, ZIN PH 1/282 in lateral view).

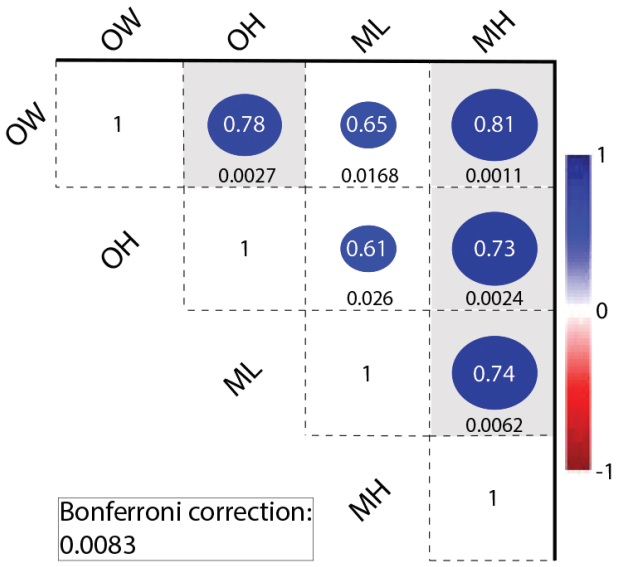

Figure 17. Correlation matrix of the studied parameters of the maxillae of *Pseudopus pannonicus*. Diagonal terms of this matrix (e.g., "OW – OW" correlation index = 1) are ignored. Terms of this matrix that are in a greyed box are statistically significant ($p < P_{Bonferroni}$). Individual p-values for each combination are shown below the corresponding correlation indexes. Abbreviations: MH: maxilla height; ML: maxilla length; OH: ornamentation height; OW: ornamentation width.

Currently, osteological studies on *P. apodus* have highlighted that the lateral surface of the maxillae of this taxon bears only light ornamentation (Klembara 1981; Klembara et al. 2017; Villa and Delfino 2019a) that is supposedly thinner and located slightly higher up on the nasal process than in *P. pannonicus*. Maxillae of *Pseudopus laurillardi* are known to exhibit various types of ornamentation, somewhat similar to the condition known in *P. pannonicus*, and more pronounced in the larger specimens (Klembara et al. 2010). This condition of the maxilla is not known for *Pseudopus ahnikoviensis* and *Pseudopus confertus*. As emphasized by Roček (2019), this character state might be of interest in distinguishing between *P. pannonicus* and *P. apodus*. If the trend observed in our material and suggested by our statistical analyses were to be confirmed by the input of new material, then hypotheses on the cause(s) of the differences in character expression between *P. pannonicus* and *P. apodus* could be made. For instance, heterochronic processes may likely be at play here. Indeed, the evolution of several features of the lower jaw, skull, and vertebral column of *P. apodus* have already been shown to be influenced by heterochronic processes (Klembara et al. 2014, 2017; Čerňanský et al. 2019).

Muscular surface of the parietal. The feature of the parietal discussed here is the relative width of the muscular surface observed in *Pseudopus pannonicus* in comparison to the overall size of the parietal. Following observations and as mentioned earlier, among *P. pannonicus* the muscular surfaces appear to be rather wide, approximately equal to the PCC-MedP distance. In comparison, among *Pseudopus apodus* the MSw is approximately equal to half the PCC-MedP distance. To summarize, the conditions observed are an MSw/PCC-MedP ratio ≈ 1.0 and an MSw/PCC-MedP ratio ≈ 0.5 for *P. pannonicus* and *P. apodus* respectively. Of the 11 parietals from our material, these data could be measured on 10 of them. To the data of these 10 specimens, the data from 16 additional parietals attributed to *P. pannonicus* were added. These data were then compared with the material of *P. apodus*.

The MSw and the PCC-MedP distances were measured (Fig. 18) and an MSw/PCC-MedP ratio was attributed to each specimen.

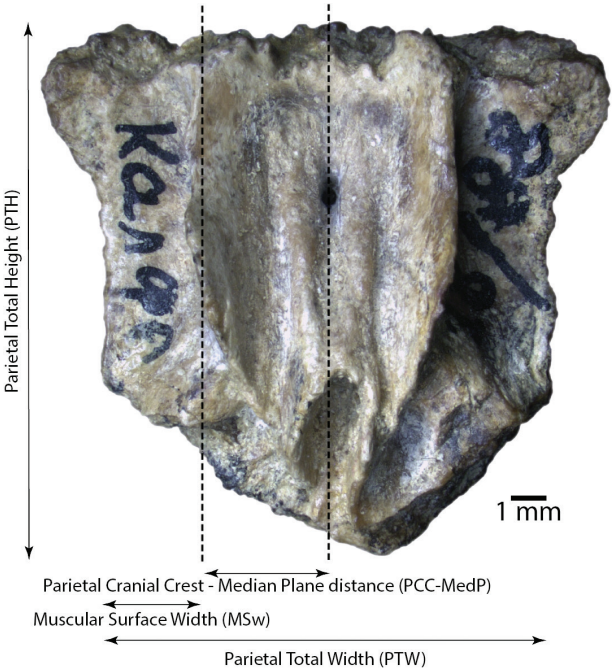

Figure 18. Measurements of the parietal of *Pseudopus pannonicus* used in statistical analyses in the present work (here, ZIN PH 18/277 in ventral view).

Following these measurements, the average ratio in *P. pannonicus* is of 0.885 (min: 0.406; max: 1.734; σ: 0.262) and the average ratio in *P. apodus* is of 0.534 (min: 0.177; max: 0.872; σ: 0.233). To determine if these ratios are significantly different from one another, a Student's *t*-test was done. The null hypothesis H_0 of this test is: "the samples are taken from a population with the given mean". The result of this test shows that the mean values of the elements sampled as *P. pannonicus* and the one of *P. apodus* are significantly different from each other (Table 1). Indeed, the sample mean (i.e., the mean ratio among *P. pannonicus*; $\bar{x} = 0.885$, N = 26) is significantly different from the given mean of 0.534 (Student's $t = 6.833$; $p_{(same\text{-}mean)} = 3.67 \times 10\text{^}{-7}$). Therefore, the null hypothesis is rejected, and it can be established that the populations (taxa) represented by the specimens are clearly distinct from one another.

Consequently, a test of correlation between these various parameters was done to evaluate the influence of body size on the relative width of the muscular surface. The correlation matrix shows, with statistical significance, that these parameters are quite strongly influenced by body size (Fig. 19). Thus, this character state presum-

Table 1. Summary of the Student *t*-test parameters regarding the parietal of *Pseudopus pannonicus* and *Pseudopus apodus*.

Samples data				
	N	**Mean**	**Std. Dev**	**Std. Error Mean**
P. apodus	6	0.534	0.233	0.095
P. pannonicus	26	0.885	0.262	0.051

t-Test results				
Mean difference	**Lower bound of the 95% confidence interval of the difference**	**Upper bound of the 95% confidence interval of the difference**	***t***	$p_{(same\ mean)}$
0.351	0.113	0.589	6.833	3.67 × 10^–7

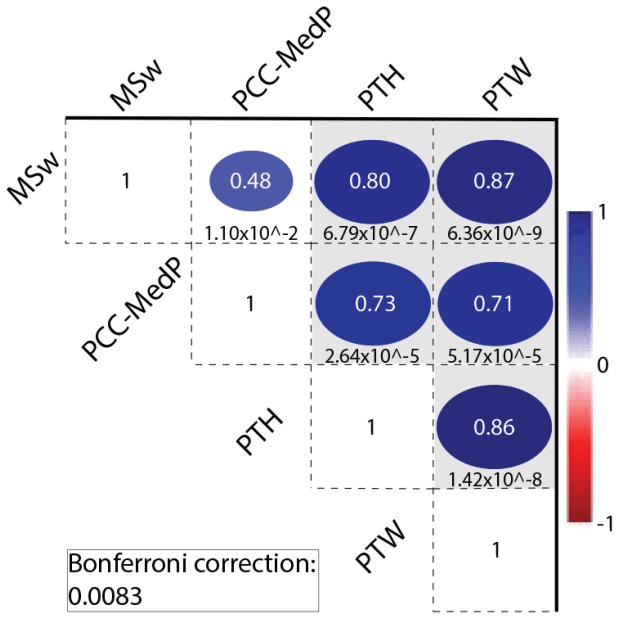

Figure 19. Correlation matrix of the studied parameters of the ventral surface of the parietal bones of *Pseudopus pannonicus*. Diagonal terms of this matrix are ignored. Terms of this matrix that are in a greyed box are statistically significant ($p < 0.05$). Abbreviations: MSw: muscular surface width; PCC-MedP: distance between the parietal cranial crest and the median plane of the parietal; PTH: parietal table height; PTW: parietal table width.

ably peculiar to *P. pannonicus* is not reliable enough to distinguish this taxon from *P. apodus*.

Vertebral elongation. As mentioned previously, the trunk vertebrae of our *P. pannonicus* material, as well as the ones described in the literature, are rather stout and compressed. These are thus quite distinct from the comparatively notably elongated trunk vertebrae of *Pseudopus apodus* (Čerňanský et al. 2019). Here, the relevance of the degree of vertebral elongation for identification purposes is examined.

The eleven presacral vertebrae from our material are here considered. To these elements, literature data from 16 additional presacral vertebrae identified as *P. pannonicus* are included. These data are then compared to the presacral vertebrae of *P. apodus*, such as the ones studied in details by Čerňanský et al. (2019). The degree of elongation of a vertebra is determined by the ratio between the centrum length and the neural arch width (i.e., CL/NAW ratio hereafter). A ratio closer to 1, or greater than 1, is equivalent to a stouter and more compressed vertebra, whereas a more elongated vertebra is associated with a ratio lesser than 1. Another assumption resides in the fact in both *P. pannonicus* and *P. apodus*, although the absolute values of both NAW and CL might very well vary throughout the relative position of a given vertebra in the column, the respective proportions of the vertebrae (i.e., the CL/NAW ratios) remain similar. It has been highlighted that the presacral vertebrae posterior to the atlas and axis of *P. apodus* display very uniform morphology despite increasing steadily in relative sizes anteroposteriorly (Hoffstetter and Gasc 1969; Čerňanský et al. 2019). Only the very first few anterior trunk vertebrae appear to diverge from this general tendency. Moreover, this tendency is seemingly not limited to *Pseudopus* or anguines as a whole. Indeed, as Hoffstetter and Gasc (1969) also pointed out, vertebrae from the presacral region of the column tend to show relative morphological uniformity among snake-like, limbless and elongated organisms. In addition, because *P. pannonicus* and *P. apodus* are admittedly similar in many regards (Fejérváry-Lángh 1923; Klembara et al. 2010, 2014, 2017; Čerňanský et al. 2019), it is not too far-fetched to expect a similar condition for such a general tendency in *P. pannonicus*.

Presacral vertebrae of *P. apodus* are quite elongated. Their ratio of elongation has been previously estimated to be about 0.62 (Čerňanský et al. 2019). The average NAW/CL ratio of the herein described presacral vertebrae is closer to 1 ($\bar{x} = 0.96$). However, there is some variability among these ratios (min = 0.79; max = 1.37; $\sigma = 0.156$). To determine whether the values of the ratios obtained for *P. pannonicus* are different from the average elongation ratio of *P. apodus*, a Student's *t*-test was conducted. The null hypothesis H_0 of this test is: "The samples are taken from a population with the given mean". The results of this test show that the elongation ratios differ significantly between these taxa (Table 2). Indeed, the sample mean ($\bar{x} = 0.96$, N = 27) is significantly different from 0.62 (Student's $t = 11.132$; $p_{(same\text{-}mean)} = 1.4768 \times 10^{-11}$). Therefore, the null hypothesis is here rejected.

Table 2. Summary of the Student *t*-test parameters of trunk vertebrae of *Pseudopus pannonicus* and *Pseudopus apodus*.

Samples data				
	N	**Mean**	**Std. Dev**	**Std. Error Mean**
P. apodus	N/A	(*)0.620	N/A	N/A
P. pannonicus	27	0.96	0.156	0.03

t-Test results				
Mean difference	**Lower bound of the 95% confidence interval of the difference**	**Upper bound of the 95% confidence interval of the difference**	***t***	$p_{(same\ mean)}$
0.34	0.278	0.402	11.132	1.4768 × 10^–11

(*): Average ratio data for *P. apodus* from Čerňanský et al. (2019). N/A: Not Available.

Following this result, the character state of "stout presacral vertebrae with reduced elongation" appears to be important for comparisons between *P. pannonicus* and *P. apodus*.

Conclusions

Here were studied and described various cranial and vertebral elements attributed to the fossil anguine *Pseudopus pannonicus*. This material originates from several localities spread across Eastern Europe and the North Caucasus. The fossiliferous deposits are spanning the Upper Cenozoic (MN 10 to MN 15 / early MN 16). This material extends our knowledge of *P. pannonicus* in several aspects. Besides taxonomical discussion, the report of the elements from the localities from the Northern Caucasus represents some of the most, if not the most, easternmost occurrences currently documented for *P. pannonicus*, pending the revision and clarification of *Ophisaurus apodus dzhafarovi* from the Pleistocene of Azerbaijan. Although with limited taxonomic implications because of the high scarcity of this particular element, we report on the first lacrimal bone known in the fossil record of this species. Several osteological features and their validity in regard to comparisons between the fossil *P. pannonicus* and the very similar extant *Pseudopus apodus* were described and discussed. This new material included a handful of caudal vertebrae that unfortunately did not provide any new meaningful insight toward potentially distinctive features among *Pseudopus* species (supposing there is any in the first place). When data were suitable, statistical analyses were performed to study the influence of body-size parameters on the expression of a set of cranial and vertebral traits. It was shown that several of these traits were rather strongly linked to body size, thus rendering them unreliable for diagnostical purposes between *P. pannonicus* and *P. apodus*. Two newly recognized traits in *P. pannonicus* in comparison to *P. apodus* are respectively related to the development of the osteodermal crust of the maxilla and the degree of elongation of the trunk vertebrae. Finally, the following three features are suggested as being diagnostic of *P. pannonicus*: (1) more strongly developed ornamentation of the nasal process of the maxilla in comparison to *P. apodus*; (2) splenial facet reaches posterior to the anterior inferior alveolar foramen – thus excluding the coronoid from this foramen; and (3) short and compressed presacral vertebrae in comparison to the more elongated vertebrae of *P. apodus*.

Acknowledgments

We thank Andrea Villa for his comments and insights regarding the influence of body-size parameters that inspired the statistical analysis section presented here. Our gratitude is also addressed towards Georgios Georgalis and Zbigniew Szyndlar of the Institute of Systematics and Evolution of Animals of the Polish Academy of Sciences for allowing loans and access to some of the comparative material of *Pseudopus pannonicus* from Poland included in Suppl. material 1 to E. L. and A. Č. We are deeply indebted to László Makádi and the Department of Collections of the Supervisory Authority for Regulatory Affairs in Budapest, Hungary, for providing E. L. access to their collections, hosting the original material in addition to comparative specimens of *Pseudopus pannonicus*, and for their precious help in the acquisition of SEM pictures of this valuable material figured in the present work. We are indebted to Jozef Klembara (Comenius University in Bratislava) for the access to CT scans of the extant *Pseudopus apodus* (DE 52). We thank Krister T. Smith (Senckenberg Research Institute, Germany) and Georgios Georgalis (Polish Academy of Sciences, Poland) for their comments and revisions on the manuscript. This work was supported by the Scientific Grant Agency of the Ministry of Education of Slovak Republic and Slovak Academy of Sciences, Grant Nr. 1/0191/21 (to A. Č), and Grant Nr. UK/49/2022 (to E. L.) and by the Zoological Institute, Russian Academy of Sciences (project 122031100282-2. The Scanning Electron Microscope used in this study, and the pictures subsequently acquired, was established thanks to the GINOP-2.3.3-15-2017-00043 grant.

References

Alekperov AM (1978) Zemnovodnye i presmykayushchiesya Azerbaydzhana [Amphibians and reptiles in Azerbaijan].

Alexejew A (1912) Description de la faune méotique des vertébrés des environs du Village Petroviérovak (District Tiraspol). I. Anguidae. Zapiski matematicheskogo otdeleniya Novorossiiskogo obshchestva. estestvoispytatelei 39: 13–40.

Augé M (2005) Évolution des lézards du Paléogène en Europe. Mémoires du Muséum national d'Histoire naturelle 192: 1–369.

Bachmayer F, Młynarski M (1977) Bemerkungen über die fossilen *Ophisaurus*-Reste von Österreich und Polen. Akademie der Wissenschaften 186: 285–299.

Bailon S (1991) Amphibiens et reptiles du Pliocène et du Quaternaire de France et d'Espagne: mise en place et évolution des faunes. Paris-Diderot.

Bailon S, Augé M (2012) Un nouveau genre, *Ragesaurus* (Squamata, Anguidae, Anguinae), du Pléistocène inférieur des îles Medas (Catalogne, Espagne). Bulletin de la Société géologique de France 183: 683–688. https://doi.org/10.2113/gssgfbull.183.6.683

Baryshnikov GF, Zakharov DS (2013) Early Pliocene bear *Ursus thibetanus* (Mammalia, Carnivora) from Priozernoe locality in the Dniester Basin (Moldova Republic). Proceedings of the Zoological Institute RAS 317: 3–10. https://doi.org/10.31610/trudyzin/2013.317.1.3

Blain H-A, Bailon S (2006) Catalogue of Spanish Plio-Pleistocene amphibians and squamate reptiles from the Museu de Geologia de Barcelona. Treballs del Museu de Geologia de Barcelona 14: 61–80.

Blain H-A, Bailon S, Agustí J (2016) The geographical and chronological pattern of herpetofaunal Pleistocene extinctions on the Iberian Peninsula. Comptes Rendus Palevol 15: 731–744. https://doi.org/10.1016/j.crpv.2015.05.008

Bolkay SJ (1913) Additions to the fossil herpetology of Hungary from the Pannonian and Praeglacial periods. Mitteilungen aus dem Jahrbuche der königlich ungarischen Geologischen Reichsanstalt 21: 217–230.

Burbrink FT, Grazziotin FG, Pyron RA, Cundall D, Donnellan S, Irish F, Keogh JS, Kraus F, Murphy RW, Noonan B (2020) Interrogating genomic-scale data for Squamata (lizards, snakes, and amphisbaenians) shows no support for key traditional morphological relationships. Systematic biology 69: 502–520. https://doi.org/10.1093/sysbio/syz062

Čermák S (2016) The Late Miocene species *Ochotona kalfense* (Mammalia, Lagomorpha) of Moldova: The oldest European record of the genus in the context of the earliest Ochotoninae. Comptes Rendus Palevol 15: 927–940. https://doi.org/10.1016/j.crpv.2016.04.010

Čerňanský A, Klembara J (2017) A skeleton of *Ophisaurus* (Squamata: Anguidae) from the middle Miocene of Germany, with a revision of the partly articulated postcranial material from Slovakia using micro-computed tomography. Journal of Vertebrate Paleontology 37: e1333515. https://doi.org/10.1080/02724634.2017.1333515

Čerňanský A, Rage J-C, Klembara J (2015) The Early Miocene squamates of Amöneburg (Germany): the first stages of modern squamates in Europe. Journal of Systematic Palaeontology 13: 97–128. https://doi.org/10.1080/14772019.2014.897266

Čerňanský A, Szyndlar Z, Mörs T (2017a) Fossil squamate faunas from the Neogene of Hambach (northwestern Germany). Palaeobiodiversity and Palaeoenvironments 97: 329–354. https://doi.org/10.1007/s12549-016-0252-1

Čerňanský A, Vasilyan D, Georgalis GL, Joniak P, Mayda S, Klembara J (2017b) First record of fossil anguines (Squamata; Anguidae) from the Oligocene and Miocene of Turkey. Swiss Journal of Geosciences 110: 741–751. https://doi.org/10.1007/s00015-017-0272-5

Čerňanský A, Yaryhin O, Ciceková J, Werneburg I, Hain M, Klembara J (2019) Vertebral Comparative Anatomy and Morphological Differences in Anguine Lizards with a Special Reference to *Pseudopus apodus*. The Anatomical Record 302: 232–257. https://doi.org/10.1002/ar.23944

Čerňanský A, Singh NP, Patnaik R, Sharma KM, Tiwari RP, Sehgal RK, Singh NA, Choudhary D (2022) The Miocene fossil lizards from Kutch (Gujarat), India: a rare window to the past diversity of this subcontinent. Journal of Paleontology 96: 213–223. https://doi.org/10.1017/jpa.2021.85

Conrad JL (2008) Phylogeny and systematics of Squamata (Reptilia) based on morphology. Bulletin of the American Museum of Natural History 2008: 1–182. https://doi.org/10.1206/310.1

Daudin FM (1803) Histoire naturelle, générale et particulière des reptiles: ouvrage faisant suite à l'histoire naturelle générale et particulière, composée par Leclerc de Buffon, et rédigée par C.S. Sonnini. Tome septième. F. Dufart. Paris, 436 pp. https://doi.org/10.5962/bhl.title.60678

Delfino M (2002) Erpetofaune italiane del Neogene e del Quaternario. Università degli Studi di Modena e Reggio Emilia.

Delinschi A (2014) Late Miocene lagomorphs from the Republic of Moldova. Annales de Paléontologie 100: 157–163. https://doi.org/10.1016/j.annpal.2013.10.004

Estes R (1983) Sauria terrestria, Amphisbaenia, Handbuch Der Paläoherpetologie, Part 10A. Gustav Fischer Verlag, Stuttgart, Germany, 249 pp.

Fejérváry-Lángh A (1923) Beiträge zu einer Monographie der fossilen Ophisaurier. Palaeontologia Hungarica 1: 123–220.

Fürbringer M (1900) Zur vergleichenden anatomie des Brustschulterapparates und der Schultermuskeln. Jenaische Zeitschrift für Naturwissenschaft 34: 215–718. https://doi.org/10.5962/bhl.title.52377

Gauthier JA (1982) Fossil xenosaurid and anguid lizards from the early Eocene Wasatch Formation, southeast Wyoming, and a revision of the Anguioidea. Rocky Mountain Geology 21: 7–54.

Gauthier JA, Kearney M, Maisano JA, Rieppel O, Behlke ADB (2012) Assembling the Squamate Tree of Life: Perspectives from the Phenotype and the Fossil Record. Bulletin of the Peabody Museum of Natural History 53: 3–308. https://doi.org/10.3374/014.053.0101

Georgalis G, Villa A, Ivanov M, Vasilyan D, Delfino M (2019a) Fossil amphibians and reptiles from the Neogene locality of Maramena (Greece), the most diverse European herpetofauna at the Miocene/Pliocene transition boundary. Palaeontologia Electronica 22.3.: 1–99. https://doi.org/10.26879/908

Georgalis GL, Scheyer TM (2021) Lizards and snakes from the earliest Miocene of Saint-Gérand-le-Puy, France: an anatomical and histological approach of some of the oldest Neogene squamates from Europe. BMC Ecology and Evolution 21: 1–22. https://doi.org/10.1186/s12862-021-01874-x

Georgalis GL, Delfino M (2022) The fossil record of lizards and snakes (Reptilia: Squamata) in Greece. In: Fossil Vertebrates of Greece Vol. 1. Springer, 205–235. https://doi.org/10.1007/978-3-030-68398-6_7

Georgalis GL, Villa A, Delfino M (2017a) Fossil lizards and snakes from Ano Metochi–a diverse squamate fauna from the latest Miocene of northern Greece. Historical Biology 29: 730–742. https://doi.org/10.1080/08912963.2016.1234619

Georgalis GL, Villa A, Delfino M (2017b) The last European varanid: demise and extinction of monitor lizards (Squamata, Varanidae) from Europe. Journal of Vertebrate Paleontology 37: e1301946. https://doi.org/10.1080/02724634.2017.1301946

Georgalis GL, Čerňanský A, Klembara J (2021) Osteological atlas of new lizards from the Phosphorites du Quercy (France), based on historical, forgotten, fossil material. Geodiversitas 43: 219–293. https://doi.org/10.5252/geodiversitas2021v43a9

Georgalis GL, Rage J-C, de Bonis L, Koufos GD (2018) Lizards and snakes from the late Miocene hominoid locality of Ravin de la Pluie (Axios Valley, Greece). Swiss Journal of Geosciences 111: 169–181. https://doi.org/10.1007/s00015-017-0291-2

Georgalis GL, Villa A, Ivanov M, Roussiakis S, Skandalos P, Delfino M (2019b) Early Miocene herpetofaunas from the Greek localities of Aliveri and Karydia – bridging a gap in the knowledge of amphibians and reptiles from the early Neogene of southeastern Europe. Historical Biology 31: 1045–1064. https://doi.org/10.1080/08912963.2017.1417404

Glavaš OJ, Počanić P, Lovrić V, Derežanin L, Tadić Z, Lisičić D (2020) Morphological and ecological divergence in two populations of European glass lizard, *Pseudopus apodus* (Squamata: Anguidae). Zoological Research 41: 172–181. https://doi.org/10.24272/j.issn.2095-8137.2020.025

Godina AY, David AI (1973) Neogenoviye mestonahozhdeniya pozvonochnyh na territorii Moldavskoy SSR [Neogene localities of vertebrates on the territory of the USSR]. Chisinau: Shtiintsa.

Gray JE (1825) A synopsis of the genera of reptiles and Amphibia, with a description of some new species. Annals of Philosophy Series 2: 193–217.

Gray JE (1853) Descriptions of some undescribed species of reptiles collected by Dr. Joseph Hooker in the Khassia mountains, East Bengal, and Sikkim Himalaya. Annals and Magazine of Natural History 12: 386–392. https://doi.org/10.1080/03745485709495063

Günther A (1873) Description of a new saurian (*Hyalosaurus*) allied to *Pseudopus*. Annals and Magazine of Natural History 11: 351–351. https://doi.org/10.1080/00222937308696828

Hammer Ø, Harper DA, Ryan PD (2001) PAST: Paleontological statistics software package for education and data analysis. Palaeontologia Electronica 4: 9.

Hoffstetter R, Gasc J-P (1969) Vertebrae and ribs of modern reptiles. Biology of the Reptilia 1: 201–310.

Holman JA (1998) Pleistocene amphibians and reptiles in Britain and Europe. Oxford University Press, New York. https://doi.org/10.1093/oso/9780195112320.001.0001

[ICZN] IC on ZN (1999) International Commission on Zoological Nomenclature. 4th ed. International Trust for Zoological Nomenclature, London, 306 pp.

Ivanov M, Čerňanský A, Bonilla-Salomón I, Luján ÀH (2020) Early Miocene squamate assemblage from the Mokrá-Western Quarry (Czech Republic) and its palaeobiogeographical and palaeoenvironmental implications. Geodiversitas 42: 343–376. https://doi.org/10.5252/geodiversitas2020v42a20

Jablonski D, Ribeiro-Júnior MA, Meiri S, Maza E, Kukushkin OV, Chirikova M, Pirosová A, Jelić D, Mikulíček P, Jandzik D (2021) Morphological and genetic differentiation in the anguid lizard *Pseudopus apodus* supports the existence of an endemic subspecies in the Levant. Vertebrate Zoology 71: 175–200. https://doi.org/10.3897/vz.71.e60800

Jandzik D, Jablonski D, Zinenko O, Kukushkin OV, Moravec J, Gvoždík V (2018) Pleistocene extinctions and recent expansions in an anguid lizard of the genus *Pseudopus*. Zoologica Scripta 47: 21–32. https://doi.org/10.1111/zsc.12256

Klembara J (1979) Neue Funde der Gattungen *Ophisaurus* und *Anguis* (Squamata, Reptilia) aus dem Untermiozän Westböhmens (CSSR). Věstník Ústředního ústavu geologického 54: 163–169.

Klembara J (1981) Beitrag zur Kenntnis der Subfamilie Anguinae (Reptilia, Anguidae). Acta Universitatis Carolinae, Geologica 2: 121–168.

Klembara J (1986) Neue Funde der Gattungen *Pseudopus* und *Anguis* (Reptilia, Anguinae) aus drei Pliopleistozänen Mitteleuropätischen Lokalitäten. Geologický zborník 37: 91–106.

Klembara J (2012) A new species of *Pseudopus* (Squamata, Anguidae) from the early Miocene of Northwest Bohemia (Czech Republic). Journal of Vertebrate Paleontology 32: 854–866. https://doi.org/10.1080/02724634.2012.670177

Klembara J (2015) New finds of anguines (Squamata, Anguidae) from the Early Miocene of Northwest Bohemia (Czech Republic). Paläontologische Zeitschrift 89: 171–195. https://doi.org/10.1007/s12542-014-0226-4

Klembara J, Rummel M (2018) New material of *Ophisaurus*, *Anguis* and *Pseudopus* (Squamata, Anguidae, Anguinae) from the Miocene of the Czech Republic and Germany and systematic revision and palaeobiogeography of the Cenozoic Anguinae. Geological Magazine 155: 20–44. https://doi.org/10.1017/S0016756816000753

Klembara J, Böhme M, Rummel M (2010) Revision of the anguine lizard *Pseudopus laurillardi* (Squamata, Anguidae) from the Miocene of Europe, with comments on paleoecology. Journal of Paleontology 84: 159–196. https://doi.org/10.1666/09-033R1.1

Klembara J, Hain M, Dobiašová K (2014) Comparative anatomy of the lower jaw and dentition of *Pseudopus apodus* and the interrelationships of species of subfamily Anguinae (Anguimorpha, Anguidae): Anatomy of lower jaw and teeth of Anguinae. The Anatomical Record 297: 516–544. https://doi.org/10.1002/ar.22854

Klembara J, Hain M, Čerňanský A (2019) The first record of anguine lizards (Anguimorpha, Anguidae) from the early Miocene locality Ulm – Westtangente in Germany. Historical Biology 31: 1016–1027. https://doi.org/10.1080/08912963.2017.1416469

Klembara J, Dobiašová K, Hain M, Yaryhin O (2017) Skull anatomy and ontogeny of legless lizard *Pseudopus apodus* (Pallas, 1775): Heterochronic influences on form. The Anatomical Record 300: 460–502. https://doi.org/10.1002/ar.23532

Koretsky IA (2001) Morphology and systematics of Miocene Phocinae (Mammalia: Carnivora) from Paratethys and the north Atlantic region. Geologica Hungarica, Series Palaeontologica 54: 1–109.

Kormos T (1911) Der Pliozäne Knochenfund bei Polgárdi. Földtani Közlöni 41: 1–19.

Kotsakis T (1989) Late Turolian amphibians and reptiles from Brisighella (northern Italy): preliminary report. Bollettino della Società paleontologica italiana 28: 277–280.

Kovalchuk O, Ferraris C (2016) Late Cenozoic catfishes of Southeastern Europe with inference to their taxonomy and palaeogeography. Palaeontologia Electronica: 1–17. https://doi.org/10.26879/616

Krakhmalnaya T (2008) Proboscideans and ungulates of Late Miocene fauna of Ukraine. In: 6th Meething of The European Association of Vertebrate Palaeontologists, 51.

Lartet E (1851) Notice sur la colline de Sansan, suivie d'une récapitulation des diverses espèces d'animaux vertébrés fossiles, trouvés soit à Sansan, soit dans d'autres gisements du terrain tertiaire du miocène dans le bassin sous-pyrénéen. J.A. Portes, Auch.

Linnaeus C (1758) Tomus 1 Systema naturæ per regna tria naturae, secundum classes, ordines, genera, species cum characteribus, differentiis, synonymis, locis. Decima. Laurentii Salvius, Stockholm, 824 pp. https://doi.org/10.5962/bhl.title.542

Loréal E, Villa A, Georgalis G, Delfino M (2020) Amphibians and reptiles from the late Miocene and early Pliocene of the Ptolemais area (Western Macedonia, Greece). Annales de Paléontologie 106: 102407. https://doi.org/10.1016/j.annpal.2020.102407

Maisano J (2003) The Deep Scaly Project, "*Ophisaurus apodus*" (Online). Digital Morphology. [Available from:] http://digimorph.org/specimens/Ophisaurus_apodus/ [December 15, 2022]

Merrem B (1820) Versuch eines systems der Amphibien. Krieger. https://doi.org/10.5962/bhl.title.5037

Meszoely CA (1970) North American fossil anguid lizards. Bulletin of the Museum of Comparative Zoology 139: 87–149.

Młynarski M (1956) Lizards from the Pliocene of Poland. Acta Palaeontologica Polonica 1: 135–152.

Młynarski M (1962) Notes on the amphibian and reptilian fauna of the Polish Pliocene and early Pleistocene. Państwowe Wydawnictwo Naukowe-Oddział Kraków.

Młynarski M (1964) Die jungpliozäne Reptilienfauna von Rebielice Królewskie, Polen. Senckenbergiana biologica 45: 325–347.

Młynarski M, Szyndlar Z, Estes R, Sanchiz B (1984) Amphibians and reptiles from the Pliocene locality of Weże II near Dzialoszyn (Polen). Acta Palaeontologica Polonica 29: 209–226.

Nadachowski A, Mirosław-Grabowska J, David A, Tomek T, Garapich A, Pascaru V, Obadă T, Szyndlar Z (2006) Faunal assemblages and biostratigraphy of several Pliocene sites from Moldova. Cour. Forsch.-Inst. Senckenberg 256: 249–259.

Obst F (1978) Zur geographischen Variabilitat des Scheltopusik, *Ophisaurus apodus* (Pallas) (Reptilia, Squamata, Anguidae). Zoologische

Abhandlungen Staatliches Museum für Tierkunde in Dresden 35: 129–140. https://doi.org/10.1515/9783112598764-002

Oppel M (1811) Die ordnungen, familien und gattungen der reptilien als prodrom einer naturgeschichte derselben. Comm. Lindauer, München, 87 pp. https://doi.org/10.5962/bhl.title.4911

Palcu DV, Vasiliev I, Stoica M, Krijgsman W (2019) The end of the Great Khersonian Drying of Eurasia: Magnetostratigraphic dating of the Maeotian transgression in the Eastern Paratethys. Basin Research 31: 33–58. https://doi.org/10.1111/bre.12307

Pallas PS (1775) *Lacerta apoda* descripta. Novi Commentarii Academiae Scientiarum Imperialis Petropolitanae 19: 435–454.

Petronio C, Krakhmalnaya T, Bellucci L, Di Stefano G (2007) Remarks on some Eurasian pliocervines: Characteristics, evolution, and relationships with the tribe Cervini. Geobios 40: 113–130. https://doi.org/10.1016/j.geobios.2006.01.002

Pyron R, Burbrink FT, Wiens JJ (2013) A phylogeny and revised classification of Squamata, including 4161 species of lizards and snakes. BMC Evolutionary Biology 13: 93. https://doi.org/10.1186/1471-2148-13-93

Rage J-C, Bailon S (2005) Amphibians and squamate reptiles from the late early Miocene (MN 4) of Béon 1 (Montréal-du-Gers, southwestern France). Geodiversitas 27: 413–441.

Redkozubov OI (2003) Pliocene and Lower Pleistocene fauna reptiles of Republic Moldova. In: 12th Ordinary General Meeting, Societas Europaea Herpetologica (SEH). Zoological Institute of the Russian Academy of Sciences, Saint-Petersburg, Russia, 138–139.

Redkozubov OI (2005) Herpetofauna of the middle-Pliocene reference location Lucheshty (Republic of Moldova). In: Problems of paleontology and archeology of the south of Russia and neighbouring territories. Materials of international conference. Rostov-on-Don: Ltd. "CVVR," 138.

Redkozubov OI (2008) Pliocene snakes of R. Moldova (Viperinae). In: Structura şi funcţionarea ecosistemelor în zona de interferenţă biogeografică. Simpozion internaţiona, 219–221.

Roček Z (1980) The dentition of the European glass lizard *Ophisaurus apodus* (Pallas, 1775) (Reptilia, Sauria: Anguidae), with notes on the pattern of tooth replacement. Amphibia-Reptilia 1: 19–27. https://doi.org/10.1163/156853880X00033

Roček Z (1984) Lizards (Reptilia: Sauria) from the Lower Miocene locality Dolnice (Bohemia, Czechoslovakia). Rozpravy Československé Akademie věd. Řada matematických a přírodních věd 93.

Roček Z (2019) A contribution to the herpetofauna from the late Miocene of Gritsev (Ukraine). Comptes Rendus Palevol 18: 817–847. https://doi.org/10.1016/j.crpv.2019.07.003

Rosina VV, Sinitsa MV (2014) Bats (Chiroptera, Mammalia) from the Turolian of the Ukraine: phylogenetic and biostratigraphic considerations. Neues Jahrbuch für Geologie und Paläontologie - Abhandlungen 272: 147–166. https://doi.org/10.1127/0077-7749/2014/0403

Schmidt WJ (1914) Studium am Integument der Reptilien. V. Anguiden. Zoologische Jahrbücher 38: 1–102.

Schneider CA, Rasband WS, Eliceiri KW (2012) NIH Image to ImageJ: 25 years of image analysis. Nature Methods 9: 671–675. https://doi.org/10.1038/nmeth.2089

Sindaco R, Jeremčenko VK (2008) 1 The Reptiles of the Western Palearctic: Annotated checklist and distributional atlas of the turtles, crocodiles, amphisbaenians and lizards of Europe, North Africa, Middle East and Central Asia. Edizioni Belvedere Latina.

Sinitsa MV, Delinschi A (2016) The earliest member of *Neocricetodon* (Rodentia: Cricetidae): a redescription of *N. moldavicus* from Eastern Europe, and its bearing on the evolution of the genus. Journal of Paleontology 90: 771–784. https://doi.org/10.1017/jpa.2016.72

Smith KT (2011) The evolution of mid-latitude faunas during the Eocene: late Eocene lizards of the Medicine Pole Hills reconsidered. Bulletin of the Peabody Museum of Natural History 52: 3–105. https://doi.org/10.3374/014.052.0101

Smith KT, Bhullar B-AS, Köhler G, Habersetzer J (2018) The Only Known Jawed Vertebrate with Four Eyes and the Bauplan of the Pineal Complex. Current Biology 28: 1101–1107.e2. https://doi.org/10.1016/j.cub.2018.02.021

Spinner M, Bleckmann H, Westhoff G (2015) Morphology and frictional properties of scales of *Pseudopus apodus* (Anguidae, Reptilia). Zoology 118: 171–175. https://doi.org/10.1016/j.zool.2014.11.002

Sullivan RM (1979) Revision of the Paleogene genus *Glyptosaurus* (Reptilia, Anguidae). Bulletin of the American Museum of Natural History 163: 1–72.

Sullivan RM (2019) The taxonomy, chronostratigraphy and paleobiogeography of glyptosaurine lizards (Glyptosaurinae, Anguidae). Comptes Rendus Palevol 18: 747–763. https://doi.org/10.1016/j.crpv.2019.05.006

Syromyatnikova E (2018) Palaeobatrachid frog from the late Miocene of Northern Caucasus, Russia. Palaeontologia Electronica: 1–16. https://doi.org/10.26879/861

Syromyatnikova E, Roček Z (2019) New *Latonia* (Amphibia: Alytidae) from the late Miocene of northern Caucasus (Russia). Palaeobiodiversity and Palaeoenvironments 99: 495–509. https://doi.org/10.1007/s12549-018-0350-3

Syromyatnikova E, Klembara J, Redkozubov O (2022) The Pliocene *Ophisaurus* (Anguidae) from Eastern Europe: new records and additions to the history of the genus and its palaeoenvironment. Palaeobiodiversity and Palaeoenvironments: 1–10. https://doi.org/10.1007/s12549-022-00556-w

Syromyatnikova E, Georgalis GL, Mayda S, Kaya T, Saraç G (2019) A new early Miocene herpetofauna from Kilçak, Turkey. Russian Journal of Herpetology 26: 205. https://doi.org/10.30906/1026-2296-2019-26-4-205-224

Syromyatnikova EV (2017a) Redescription of *Pelobates praefuscus* Khosatzky, 1985 and new records of *Pelobates* from the late Miocene–Pleistocene of Eastern Europe. Historical Biology 31: 888–897. https://doi.org/10.1080/08912963.2017.1402015

Syromyatnikova EV (2017b) Two pelobatid frogs from the Late Miocene of Caucasus (Russia). Palaeontologia Electronica 20: 1–12. https://doi.org/10.26879/772

Szyndlar Z (1984) Fossil snakes from Poland. Acta Zoologica Cracoviensia 28: 1–156.

Szyndlar Z (1991a) A review of Neogene and Quaternary snakes of Central and Eastern Europe. Part I: Scolecophidia, Boidae, Colubrinae. Estudios Geológicos 47: 103–126. https://doi.org/10.3989/egeol.91471-2412

Szyndlar Z (1991b) A review of Neogene and Quaternary snakes of Central and Eastern Europe. Part II: Natricinae, Elapidae, Viperidae. Estudios Geológicos 47: 237–266. https://doi.org/10.3989/egeol.91471-2412

Tempfer PM (2009) The early Vallesian vertebrates of Atzelsdorf (Late Miocene, Austria). 3. Squamata, Scleroglossa. Annalen des Naturhistorischen Museums in Wien 111: 489–498.

Tesakov AS, Titov VV, Simakova AN, Frolov PD, Syromyatnikova EV, Kurshakov SV, Volkova NV, Trikhunkov YI, Sotnikova MV, Kruskop SV, Zelenkov NV, Tesakova EM, Palatov DM (2017) Late Miocene (Early Turolian) vertebrate faunas and associated biotic record of the Northern Caucasus: Geology, palaeoenvironment, biochronology. Fossil Imprint 73: 383–444. https://doi.org/10.2478/if-2017-0021

Vasile Ștefan, Venczel M, Petculescu A (2021) Early Pleistocene amphibians and squamates from Copăceni (Dacian Basin, southern Romania). Palaeobiodiversity and Palaeoenvironments 101: 967–983. https://doi.org/10.1007/s12549-020-00465-w

Vasilyan D, Čerňanský A, Szyndlar Z, Mörs T (2022) Amphibian and reptilian fauna from the early Miocene of Echzell, Germany. Fossil Record 25: 99–145. https://doi.org/10.3897/fr.25.83781

Venczel M (2006) Lizards from the late Miocene of Polgárdi (W-Hungary). Nymphaea 33: 25–38.

Villa A, Delfino M (2019a) A comparative atlas of the skull osteology of European lizards (Reptilia: Squamata). Zoological Journal of the Linnean Society 187: 829–928. https://doi.org/10.1093/zoolinnean/zlz035

Villa A, Delfino M (2019b) Fossil lizards and worm lizards (Reptilia, Squamata) from the Neogene and Quaternary of Europe: an overview. Swiss Journal of Palaeontology 138: 177–211. https://doi.org/10.1007/s13358-018-0172-y

Zerova GA (1993) Late Cainozoic localities of snakes and lizards of Ukraine. Revue de Paléobiologie 7: 273–280.

Zerova GA, Lungu AN, Chkhikvadze VM (1987) Large fossil vipers from northern Black Seaside and Transcaucasus. Trudy Zoologicheskogo Instituta 158: 89–99.

Zheng Y, Wiens JJ (2016) Combining phylogenomic and supermatrix approaches, and a time-calibrated phylogeny for squamate reptiles (lizards and snakes) based on 52 genes and 4162 species. Molecular Phylogenetics and Evolution 94: 537–547. https://doi.org/10.1016/j.ympev.2015.10.009

Supplementary material 1

List of the *Pseudopus pannonicus* fossil specimens used for comparative purposes

Authors: Erwan Loréal, Elena V. Syromyatnikova, Igor G. Danilov, Andrej Čerňanský

Data type: table (Excel file)

Link: https://doi.org/10.3897/fr.26.100059.suppl1

Supplementary material 2

List of the *Pseudopus apodus* specimens used for comparative purposes

Authors: Erwan Loréal, Elena V. Syromyatnikova, Igor G. Danilov, Andrej Čerňanský

Data type: table (Excel file)

Link: https://doi.org/10.3897/fr.26.100059.suppl2

Supplementary material 3

Detailed measurements and statistical data for each studied elements

Authors: Erwan Loréal, Elena V. Syromyatnikova, Igor G. Danilov, Andrej Čerňanský

Data type: tables (Excel file)

Link: https://doi.org/10.3897/fr.26.100059.suppl3